Am J Cancer Res 2022;12(1):17-47
www.ajcr.us /ISSN:2156-6976/ajcr0139787

Original Article

Modulation of BRCA1 mediated DNA damage repair by deregulated ER-α signaling in breast cancers

Arathi Rajan[1,3], Geetu R Varghese[1], Induprabha Yadev[2], Jaimie Anandan[2], Neetha R Latha[1], Dipyaman Patra[1], Neethu Krishnan[1], Krithiga Kuppusamy[1], Arathy V Warrier[1], Satej Bhushan[1], Revathy Nadhan[1,4], Ram Mohan Ram Kumar[1], Priya Srinivas[1]

[1]Cancer Research Program, Rajiv Gandhi Centre for Biotechnology, Thiruvananthapuram 695014, Kerala, India; [2]Goverment Medical College, Thiruvananthapuram 695011, Kerala, India; [3]Department of Biotechnology, University of Kerala, Thiruvananthapuram 695011, Kerala, India; [4]OU Health Stephenson Cancer Centre, Oklahoma, United State

Received October 13, 2021; Accepted November 16, 2021; Epub January 15, 2022; Published January 30, 2022

Abstract: BRCA1 mutation carriers have a greater risk of developing cancers in hormone-responsive tissues like breasts and ovaries. However, this tissue-specific incidence of BRCA1 related cancers remains elusive. The majority of the BRCA1 mutated breast cancers exhibit typical histopathological features of high-grade tumors, with basal epithelial phenotype, classified as triple-negative molecular subtype and have a higher percentage of DNA damage and chromosomal abnormality. Though there are many studies–relating BRCA1 with ER-α (Estrogen receptor-α), it has not been reported whether E2 (Estrogen) -ER-α signaling can modulate the DNA repair activities of BRCA1. The present study analyzes whether deregulation of ER-α signaling, arising as a result of E2/ER-α deficiency, could impact the BRCA1 dependent DDR (DNA Damage Response) pathways, predominantly those of DNA-DSB (Double Strand break) repair and oxidative damage response. We demonstrate that E2/E2-stimulated ER-α can augment BRCA1 mediated high fidelity repairs like HRR (Homologous Recombination Repair) and BER (Base Excision Repair) in breast cancer cells. Conversely, a condition of ER-α deficiency itself or any interruption in ligand-dependent ER-α transactivation resulted in delayed DNA damage repair, leading to persistent activation of γH2AX and retention of unrepaired DNA lesions, thereby triggering tumor progression. ER-α deficiency not only limited the HRR in cells but also facilitated the DSB repair through error prone pathways like NHEJ (Non Homologous End Joining). ER-α deficiency associated persistence of DNA lesions and reduced expression of DDR proteins were validated in human mammary tumors.

Keywords: ER-α, BRCA1, DNA damage repair, double-strand break (DNA-DSB), homologous recombination repair (HRR)

Introduction

Persistent DNA damages and defective DNA repair can activate oncogenes, inactivate tumor suppressor genes and generate genomic instability in proliferating cells, gradually leading to tumorigenesis. Inheritance of such defective genes increases the risk of cancers, as typically observed in cases of BRCA1 mutated breast/ovarian cancers. BRCA1 is a 220 kDa protein with several functional domains interacting with numerous other proteins to regulate its functions in cellular processes like DNA repair, protein ubiquitination, transcriptional activation, cell cycle regulation, and chromatin remodeling [1]. BRCA1 is associated with various DDR pathways and has a crucial role in DNA-DSB repair, promoting HRR. Therefore, this protein is ubiquitously needed by all the cells. However, BRCA1 mutation carriers have a greater risk of developing cancers in hormone-responsive tissues like breasts and ovaries; although the tissue specific incidence of BRCA1 mutated cancers remains elusive [2]. The majority of BRCA1 mutated breast cancers are of the triple-negative breast cancer (TNBC) molecular subtype, which does not express ER, PR and HER2. Mammalian cells express two types of ERs:

ER-α and ER-β. ER-α and ER-β have structural similarities and are activated by similar ligands yet are functionally distinctive. Moreover, only ER-α knockout studies have been shown to impact mammary development resulting in curtailed duct elongation, indicative of its significant role in regulating breast tumorigenesis compared to ER-β. BRCA1 is reported to inhibit ER-α, either by directly interacting with ER-α, by suppressing the ER-α co-activator p300 or by mono-ubiquitinating ER-α. Nevertheless, excess estrogen can cause ROS mediated DNA damage which can subsequently augment BRCA1 transcription [5]. BRCA1 might also have control over the differentiation of ER-α^- basal progenitor cells to ER-α^+ luminal cells, possibly explaining the ER-α negativity in BRCA1 mutated tumors [2]. It has also been identified that there are two separate contact points for ER-α in BRCA1 protein, one within aa 1-100 and the other within aa 101-200 of BRCA1; and that each of these BRCA1 peptides interact with ER-α *in vitro* and *in vivo*. Moreover, the N-terminus of BRCA1, aa 1 to 100 and aa 101 to 200 regions are also reported to accumulate at DSBs [6]. Thus, BRCA1-ER-α interaction may have a role to play in DSB repair. Traditionally ER-α signaling is not typically thought to impact DDR and studies concentrated on its classical roles of growth and proliferation.

Recently, there are reports suggesting that ER-α signaling could impact DNA damage processing through regulation of major DDR effectors like ATR, ATM, DNA-PK, BRCA1, BRCA2 and p53 [7, 8] and thereby, regulating the canonical DNA repair pathways like NHEJ, HRR, MMR (Mis-Match Repair), BER and NER (Nucleotide Excision Repair) [9-11]. Thus, we hypothesize that there exists a cross-regulatory network between ER-α signaling and DDR pathways in E2 responsive cells. Thus deregulation of E2-ER signaling arising as a result of BRCA1 mutation or ER-α haploinsufficiency would adversely affect DDR leading to tumorigenesis

Our present study analyzes whether the deregulation of ER-α signaling, arising from either BRCA1 mutation or ER-α deficiency impact the BRCA1 dependent DDR pathways, predominantly those of HRR and BER. We have demonstrated that E2 or E2 stimulated ER-α can modulate BRCA1 mediated high fidelity repairs like HRR and BER pathways, which might explain the delayed DNA damage repair ability of ER-α^- breast cancer cells.

Materials and methods

Cell lines and transfections

Breast cancer cell lines MCF-7, MDA-MB-231, T47D, obtained from ATCC, were maintained in DMEM (Gibco) with 10% Fetal Bovine Serum (Pan Biotek) at 37°C in a CO_2 incubator. HCC1937 and HCC1937wt/BRCA1(HCC1937 with wild-type BRCA1) were kind gift from Dr. Grant McArthur, Peter MacCallum Cancer Centre, VIC, Australia; maintained in RPMI (Pan Biotek) with 10% FBS at 37°C in a CO_2 incubator. Short tandem repeat profiling (STR) has been conducted to authenticate the cell lines and all the cells were periodically tested for mycoplasma infection (See Figure S6 for details of mycoplasma detection PCR). For generation of stable cell lines specific shRNA plasmids or pDNAs were used. Transfections were performed with lipofectamine LTX-PLUS/3000 (Invitrogen, #15338-100, # L3000008), the stable clones were selected using 200 µg/ml of G418 (Gibco, 10131-035) or 2-5 µg of puromycin dihydrochloride (Sigma, # P8833) for 45 days.

Tissue samples and immunohistochemical analysis (IHC)

FFPE sections of treatment naive human mammary tumor and adjacent normal tissues were obtained from Govt. Medical College, Thiruvananthapuram, Kerala, India as per ethical guidelines (HEC No: 07/13/2019/MCT & IHEC/1/2019/13). Immunohistochemical analysis was carried out using SS-Polymer HRP IHC Detection System (Biogenex #QD 400-60KE). The slides were viewed and imaged under light microscope.

DNA damage induction

Fresh stocks of cisplatin (cis-diamminedichloroplatinum (II), Sigma #P4394) were prepared by reconstituting 1 mg/ml cisplatin with 0.9% sterile saline and sub-stocks of micro molar concentrations were prepared using 2.5% DMEM. Exponentially growing cells were treated with 5 µM cisplatin for 2 hours for inducing repairable DNA-DSB. For repair assays, cisplatin treated cells were washed with sterile 1X PBS and incubated in complete growth media for 0-72

hours, as post treatment recovery/rescue. Cells maintained in 2.5% DMEM served as the control. For assays that scored estrogenic activity, cultured cells were grown in phenol red free DMEM/PRFM (Sigma, #D2905) with 5% charcoal treated FBS (CTS) (PanBiotek, #P30-2301). Oxidative damages were introduced in exponentially growing cells using 300 μM H_2O_2, for 30 minutes. 30% V/V H_2O_2 (Sigma Aldrich) was diluted in 2.5% growth media; For rescue, treated cells were washed with sterile 1X PBS and incubated in complete growth media for 0-48 hours, as post treatment recovery/rescue.

Gene MANIA analysis

The enriched list of DDR proteins belonging to different canonical mammalian repair pathways interacting with both BRCA1 and ER-α in common was obtained using GeneMANIA (http://genemania.org) analysis. GeneMANIA provides association data, domain similarity, protein interaction and co-localization data using a wealth of genomics and proteomics data. The large list of DDR genes obtained on analysis was further enriched with regard to the canonical DDR pathways.

Estrogen deprivation and tamoxifen/SCR pyrazine treatment

Prior to estradiol and tamoxifen treatments, cells were grown in 5% PRFM, exponentially growing cells were treated with 10 nM 17-β Estradiol (Sigma, #CAS 50-28-2) or 5 μM tamofixen citrate (Sigma, #T9262) for 12 hours. SCR-7 pyrazine (Sigma Aldrich, #SML1546-5MG) was used at a concentration of 30 μM for NHEJ inhibition assays.

Immuncytochemistry and co-immunoprecipitation

Immunocytochemical analysis was done as described elsewhere [12]. Briefly, cells were fixed with Acetone: Methanol at -20°C, blocked with 3% Bovine Serum Albumin (Sigma Aldrich, USA) in PBST and incubated with primary antibodies overnight. Further, after removing unbound antibodies with 1X PBS, incubated with flurochrome conjugated secondary antibodies. Cells were then counterstained with nuclear stain DAPI (Sigma aldrich). Observed under Olympus FV 300 confocal microscope (Tokyo, Japan) and processed using Nikon NIS-Elements software. (The DSB induced foci in cells were counted manually. Mean of equivalent number of foci per cell was counted, 30 cells were counted in a field and 10 fields were counted per sample).

For immunoprecipitation assays, the cells (~5×10^6) were lysed in 500 μl of lysis buffer (50 mM Tris, 300 mM, 0.4% NP40, NaCl pH 8.0, 10 mM $MgCl_2$) containing protease and phosphatase inhibitor cocktails (CST) and 1 mg of total protein was immunoprecipitated for 1 h at 4°C with IP specific antibodies. Further, protein lysate was mixed with protein A/G beads (17-5280-01, GE Healthcare) and kept overnight at 4°C at shaking. The samples were denatured by heating with laemmli sample buffer (161-0737, Biorad) containing β-mercaptoethanol for 5 min. The supernatant was then resolved using a 10% SDS-polyacrylamide gel and immunoblotting was done with IP specific antibodies.

Real time PCR

Total RNA was extracted using RNeasy kit (Qiagen). Real-time quantitative PCR was performed to quantify the relative abundance of select genes using the SensiFAST™ SYBR® No-ROX Kit (Bioline) as recommended by the manufacturers on a Biorad CFX96 real-time PCR system. Primers used in the study are listed in Table S3. GAPDH was used as endogenous control. Data was analyzed using Microsoft Excel. Mean fold change was expressed as normalized fold expression over control and plotted using GraphPad Prism 8.

Chromosome harvesting of adherent cells (metaphase spread)

Cisplatin treated ER-α deficient and proficient cells were arrested at metaphase using 1 ug/ml Karyomax colcemide (Gibco, #15210040). Post incubation, cells were trypsinized and metaphase spreads were prepared as per JoVe protocol [13] for chromosome analysis. Spreads were stained with DAPI before being imaged under fluorescent microscope.

Colony formation assay (CFA)

To analyze the effect of exogenously induced site specific DSB, on colonigenic ability of

the cells, CFA was performed as per standard protocol. For the assay, treated cells were trypsinized, washed with 1X PBS and seeded at a density of 1000 cells per well in 6 well plate and incubated at 37°C. And the cells were assessed for colony formation for about 14-21 days. Untreated or mock transfected cells maintained in complete growth media served as controls for the assay. After specified incubation period, colonies were washed and fixed with methanol: acetic acid (3:1) for 15 min at RT and stained with crystal violet for 20 min. Colonies were microscopically examined and a colony with a minimum of 50 cells was considered for quantification. Colonies were counted manually and graph was plotted using GraphPad Prism 8.

Neutral comet assay

Neutral comet assay was performed on 5 μM cisplatin treated and untreated cells, as described previously with slight modifications [14]. Briefly, exponentially growing cells were exposed to 5 μM cisplatin, for 2 hours; post-incubated in complete growth media for the indicated time periods. Trypsinized cells were then washed and re-suspended in ice-cold 1X PBS. Cell suspension (15 μl) was embedded in 120 μl of low-melting point agarose (0.5% in dH_2O at 37°C) and transferred onto agarose-coated (1.5% in PBS) slides and then the slides were allowed to dry. These spreads were then submersed in ice cold lysis buffer (10 mM Tris-HCl, 100 mM EDTA, 2.5 M NaCl, and 1% Na-laurylsarcosine, pH=7.5); for 1 h. (1 h before use 1 ml Triton X-100 and 10 ml DMSO/100 ml were added). Slides were electrophoresed in cold neutral buffer (90 mM boric acid, 90 mM Tris, 2 mM EDTA, pH= 7.5) at 0.7 V/cm for 13-20 min at 4°C. Post electrophoresis the slides were rinsed using distilled water and fixed with 100% ethanol for 30 min. Fixed slides were allowed to air dry, and were further stained with propidium iodide (50 μg/ml). Images were taken using Olympus IX70 inverted microscope.

Cell cycle analysis

After specific treatments, breast cancer cells, were trypsinized and re-suspended in 1X PBS and fixed with 70% ethanol-PBS for 30 min at 4°C. Fixed cells were washed with 1X PBS to remove traces of ethanol and further incubated with RNase at 37°C for 30 min. Finally, the cells were stained with propidium iodide (PI) containing staining solution at 37°C for 30 min. Samples were analyzed using flow cytometry (BD FACS AriaIII).

Homologous recombination assay (HR)

Cells were exposed to HR assay as per Norgen's Homologous Recombination Assay Kit protocol (Norgen biotek; #35600). Briefly, the defective dl1 and dl2 (named after the defective lacZ gene) plasmids were co-transfected into the cell and allowed to recombine upon incubation for about 12-36 hours, the recombinant products were isolated and amplified using the specific Assay/Universal primes. Assay primers detects the HR product while, universal primer detects the backbone plasmids. Amplicons were separated on 1% Agarose gel and band intensity was normalized with respect to the backbone plasmids, dl1 and dl2.

DR-GFP based HR-NHEJ assay

Cells were stably transfected using Lipofectamine-3000 as suggested by the manufacturer (Invitrogen) with 2 ug of circular pDR-GFP (Plasmid 26475, AddGene, USA); stable Puromycin-resistant colonies were selected with 2 to 6 μg/ml puromycin (Sigma). Selected DR-GFP cells were maintained in 10% fetal bovine serum (Gibco) containing DMEM. This recombination assay depends on the two inactivated tandem repeats of DR-GFP plasmid developed by M. Jasin [15] and was done as described elsewhere [16]. (Detailed in Figure S4B).

Cell free in vitro NHEJ

Standard cell free *in vitro* NHEJ was performed as described previously with few modifications [17]. Restriction digestion using EcoRI (NEB, R3101S) was used to generate plasmid substrate with cohesive ends. The linearized plasmids were purified using QIAquick gel extraction kit (Qiagen). 250 ng of the purified and linearized plasmid substrate was incubated with 1 μg of nuclear extracts from cisplatin treated MCF-7 and MDA-MB-231 cells in fresh end joining reaction buffer (10× NHEJ buffer -200 mM HEPES pH 7.5 at RT, 100 mM $MgCl_2$, 800 mM KCL, & 1 mM ATP) in a 30 μL reaction volume for 1 h at 37°C. The reaction mixture was deproteinized with proteinase K (1 mg/ml) at 65°C

for 30 min. The mixture was then purified and separated on 0.7% agarose gel for 2 hours at 60 V. DNA was detected using a Gel Doc imaging system (Bio Rad Labs.) after staining with ethidium bromide. End joining activity was measured, and is expressed as end-joining efficiency [18].

Proximity ligation assay (PLA)

In Situ PLA was performed in DSB induced MCF-7 cells, as well as in FFPE sections of human breast tumor tissues using Duo link in situ proximity ligation assay starter kit, (Sigma # DUO92101) with specific antibodies. Fluorescent red spots, indicative of the interaction between ER-α and BRCA1, at close proximity were imaged under Olympus FV 300 confocal microscope.

Briefly, a pair of secondary antibodies labeled with oligonucleotide (PLA probes), will generate signal only when they are bound in close proximity. If the two primary antibodies bind to the sample or target proteins in close proximity (at distances < 40 nm), the complementary PLA probes bound to these primary antibodies will also come in close proximity. The oligonucleotide arm of one of the PLA probes acts as a template for a rolling-circle amplification (RCA) reaction and using this ligated circle as a template, a concatemeric (repeated sequence) product is generated on amplification. The fluorescently labeled oligonucleotides will hybridize to the RCA product. The signal is visible as a distinct fluorescent spot on fluorescence microscopy.

Oligonucleotide-based incision assay (BER assay)

BER or the cleavage activity of ER-α deficient and proficient cells was analyzed using modified FAM labeled oiligos as per Saha et al. protocol, with minor modification [19]. Nuclear extracts from H_2O_2 treated cells were used for the assay. Oligos with single damaged base, 8-OXO-G were synthesized, whereas, oligos having normal bases in place of modified bases were used as controls (Detailed in Table S3). 2.5 pmol of annealed wild type as well as 8-OXO-G oligo duplexes were incubated to enable cleavage in inscision assay buffer at 37°C for 60 mins. Reaction was stopped by incubating the mixture with 0.2% SDS and 0.1 mg/ml proteinase K at 56°C for 10 min. Phenol-chloroform extraction was used to remove the proteins and the products were then separated on 20% polyacrylamide gel with 7 M urea at 15 W for ~80 min. This Urea formamide gel was imaged using Imager (azure biosystems). Products bands were quantified with relative to the sum of substrate and product bands, and expressed as a percentage value [20].

Primer sequences, shRNA sequences, pDNAs and primary antibodies used in this study are listed in Tables S2, S3 and S4.

Statistical analysis

All experiments were performed in triplicates and expressed as mean ± SD from at least three independent experiments. Error bars are given on the basis of calculated SD values. Two tailed student's t-test or ANOVA were used to test the probability of significant differences between different experimental groups. Statistical analyses were performed using GraphPad Prism 8 (USA). *P≤0.05 was considered statistically significant.

Results

BRCA1 and ER-α interact with DDR proteins

We first checked whether ER-α could interact with DDR proteins that are in turn associated with BRCA1 mediated DDR pathways, by performing analysis using the GeneMANIA online tool [21]. This network integration algorithm predicted gene association and functions including protein and genetic interactions, co-expression, co-localization, pathways and protein domain similarity between the given input genes-ESR1 and BRCA1. The analysis considered a large network of DDR specific genes belonging to the five canonical mammalian DNA repair pathways. On analysis, 19 DDR genes were found in direct association with both BRCA1 and ER-α. Of the 19 DDR genes, 6 were associated with BER and 7 with NER, 3 with MMR, 2 with HRR and 1 with NHEJ pathway (Table S1). These interactions signify the association of ER-α in DDR pathways and thus the role ER-α activity in BRCA1 regulated mammalian DNA damage repair pathways is a definite possibility.

ER-α modulates DNA-DSB repair in breast cancer cells

BRCA1 and the BRCA1 associated surveillance complex is reported to function in all the major pathways of DDR [22], but have a major role in repairing DNA-DSBs via homologous recombination. Thus, to analyze the role of ER-α in BRCA1 mediated DSB repair, we exogenously induced DNA-DSBs in breast cancer cell lines by using cisplatin (Cis-diaminodihydro-platinumchloride II). Cisplatin can generate a range of nuclear lesions including DNA-DSBs. The DSBs generated were analyzed by scoring the nuclear localization and expression of phosphorylated H2AX (γH2AX S^{139}, a hallmark for DNA-DSBs), both by ICC and western blot analysis. Out of the several concentrations tested, treatment with 5 μM cisplatin for 2 hours was found to be the lowest dosage that could induce detectable DNA-DSBs in MCF-7 cells (Figure S1A-D). Moreover, the expression of DSB repair proteins p-CHK2 and RAD51 were found to be elevated in MCF-7 cells in response DNA-DSB induction (Figure S1E-G), indicating that there is an activation of DSB repair pathways after cisplatin treatment. Interestingly upon rescue (removal of cisplatin and incubating the cells in complete growth media), the γH2AX foci and the comet tails disappeared gradually within 48 hours (**Figure 1A**). The effect of 5 μM cisplatin on cell viability was assessed by MTT and trypan blue staining assays. We observed that treatment of 5 μM cisplatin for 2 hours did not result in significant cell death (**Figure 1B-D**) but induced repairable DSBs in MCF-7 cells.

To uncover the possible role of ER-α in DSB repair we initially analyzed the expression of ER-α in response to DSB. We observed an over-expression of ER-α along with BRCA1, both at mRNA and protein levels in MCF-7 cells (**Figure 1E-I**). However, the post-treatment rescue in complete media gradually decreased the expression of BRCA1 as well as ER-α. Similar results were obtained with the breast adenocarcinoma cell line, T47D (**Figure 1J**, **1K**). Together, these signify the possible role of ER-α in BRCA1 mediated DNA-DSB repair. (See Figure S1H, S1I for cell proliferation assay post 5 μm cisplatin treatment in MDA-MB-231 and T47D cells).

Increase in BRCA1 expression both at protein and mRNA level in response to nuclear damages is previously reported [23, 24]. However, an increase in expression of ER-α in response to damage and gradual decrease in its expression on rescue was unforeseen. Thus to rule out the precise role of ER-α in DSB repair, we stably knocked down ER-α in MCF-7 cells with shRNA (See Figure S2A-C for confirmation of ER-α knockdown); and further analyzed the time dependent γH2AX kinetics. In wild-type MCF-7 cells, the γH2AX intensity and number of foci peaked in response to DNA-DSB activation and then reduced to normal after 72 hours of rescue in complete media in a time dependent manner indicating that the cells are capable of repairing their DNA in response to cisplatin induced DNA-DSB (**Figure 2A-D**).

On the contrary, in MCF-7shER-α cells the γH2AX kinetics was impaired and there was persistent activation of γH2AX even at 72 hours of post-damage rescue (**Figure 2E-H**). This was further validated with ER-$α^-$ and BRCA1 wild type MDA-MB-231 cells, exhibiting a delayed damage repair with persistent activation of γH2AX (**Figure 2I-L**). Thus, even though the cells were wild-type for BRCA1, ER-α deficiency delayed the DSB repair events in these cells.

Retention of DSB induced γ-H2AX foci for more than 24 hours is considered to be an indication of impaired DNA repair. Substantiating this hypothesis, we could observe that the ER-$α^-$ treatment naive human breast cancer tissues also showed significantly higher γH2AX expression in comparison with the ER-$α^+$ tissues in IHC analysis (**Figure 3A**). In brief, deficiency of ER-α resulted in persistent activation γH2AX and delayed the DSB repair in breast cancer cells.

The γH2AX kinetics of BRCA1 knockdown MDA-MB-231 cells (MDA-MB-231shBRCA1) which is an ER-$α^-$ cell line, (see Figure S2D, S2E for confirmation of BRCA1 knockdown) in response to cisplatin induced DSB was similar to their BRCA1 wild type controls. The cisplatin treatment resulted in aberrant γH2AX kinetics and the cells retained the damage response foci up to 48 hours of rescue time, indicative of a delayed damage repair (**Figure 3B**, **3C**). However, replicating the experiment in T47D (ER-$α^+$/BRCA1 wild-type) cells showed efficient damage repair analogous to MCF-7 cells (**Figure 3B**, bottom panel, C) indicating that BRCA1 might require functional ER-α for its repair functions.

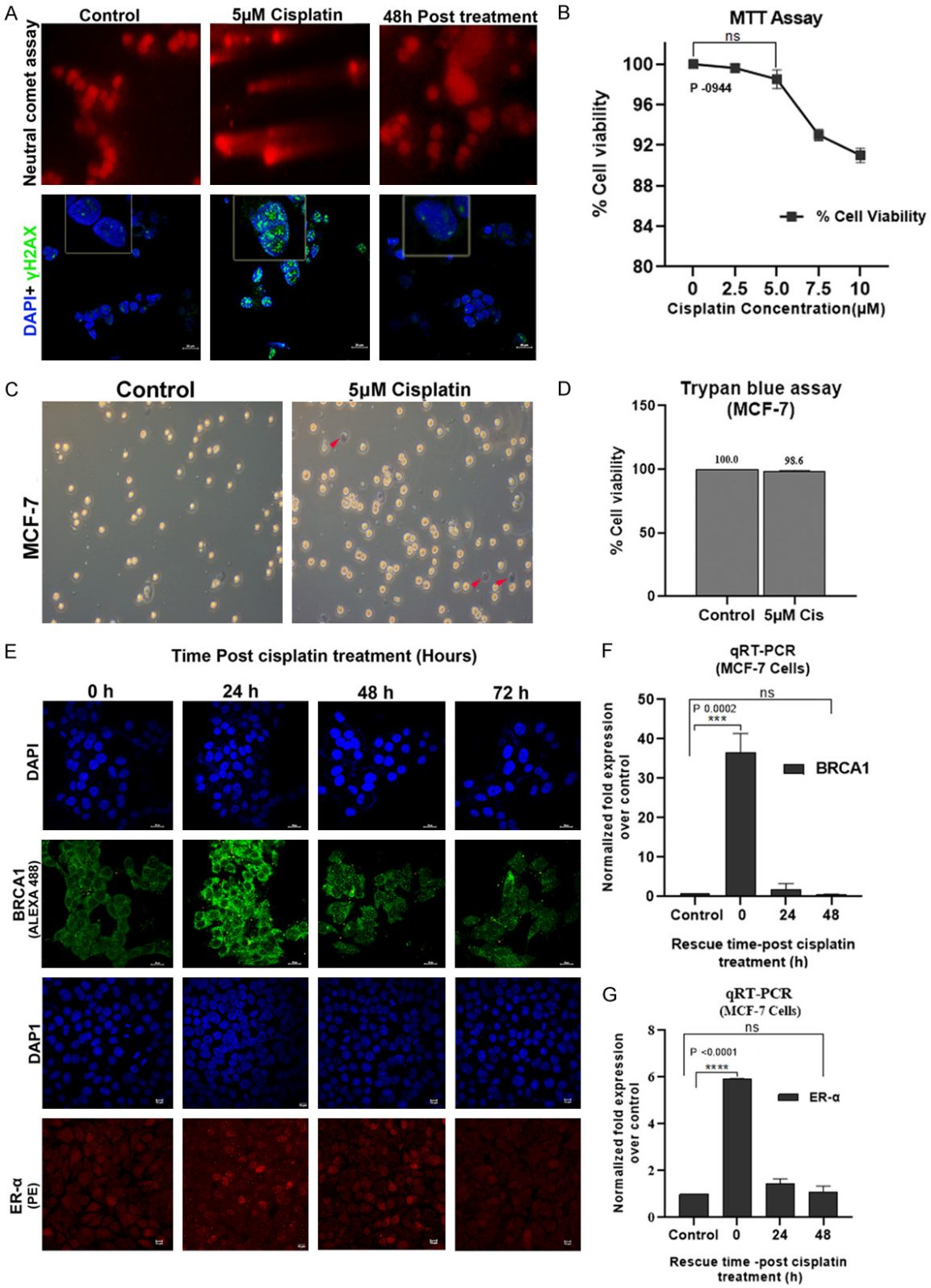
A
Control
5μM Cisplatin
48h Post treatment
Neutral comet assay
DAPI+ γH2AX
B
MTT Assay
ns
P -0944
% Cell viability
% Cell Viability
Cisplatin Concentration(μM)
C
Control
5μM Cisplatin
MCF-7
D
Trypan blue assay
(MCF-7)
% Cell viability
100.0
98.6
Control
5μM Cis
E
Time Post cisplatin treatment (Hours)
0 h
24 h
48 h
72 h
DAPI
BRCA1
(ALEXA 488)
DAP1
ER-α
(PE)
F
qRT-PCR
(MCF-7 Cells)
ns
P 0.0002
***
BRCA1
Normalized fold expression over control
Control
0
24
48
Rescue time-post cisplatin treatment (h)
G
qRT-PCR
(MCF-7 Cells)
ns
P <0.0001
****
ER-α
Normalized fold expression over control
Control
0
24
48
Rescue time -post cisplatin treatment (h)

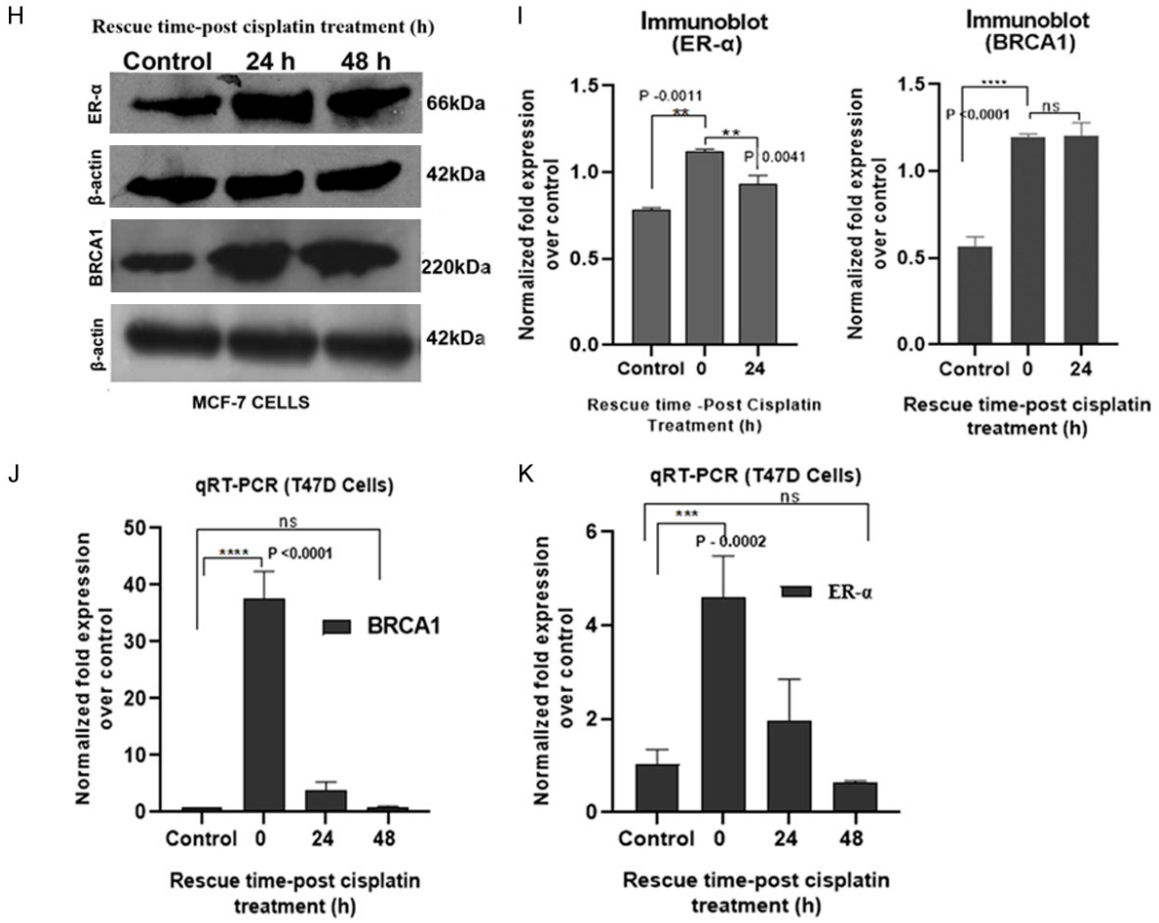

Figure 1. 5 μM cisplatin induces repairable DSBs and triggers its repair with over-expression of BRCA1 and ER-α. A. Comet tails (Top panel) and expression of phosphorylated H2AX-S139 (γH2AX) (Bottom panel) observed in response to cisplatin (5 μM/2 hours) induced DNA DSB and post treatment rescue (0 h-48 h), in MCF-7 cells. (20X, Scale bar 20 μm). Once the Cisplatin concentration of 5 μM/2 hours was found to be the least concentration to induce DSB, an MTT assay performed to assess the cell viability. B. Cell proliferation in MCF-7 assessed post 5 μM cisplatin induced DNA-DSB by MTT assay. C, D. Trypan blue exclusion staining of MCF-7 cells upon 5 μM cisplatin induced DNA-DSB. E-G. Protein/mRNA expression of BRCA1 and ER-α, scored at different time points of rescue-post DNA-DSB induction in MCF-7 cells. H, I. Western blot analysis of ER-α and BRCA1 upon DNA-DSB induction and post treatment rescue, scored at different time points in MCF-7 cells. J, K. mRNA expression of BRCA1 and ER-α in DNA-DSB induced T47D cells. (All the experiments were performed in triplicates; qRT-PCR data represents mean fold change with regard to untreated controls and are normalized to GAPDH). (Error bars, Mean ± SD, $^{*}P\leq0.05$ and $^{**}P\leq0.005$ and as $^{***}P\leq0.001$, $^{****}P\leq0.0001$-Unpaired t-test). (The extra nuclear DAPI observed with **Figure 1E** could be an over exposure or over loaded DAPI, which is usually observed with the use of DAPI containing mounting media).

For further validations, the same experiment was repeated in isogenic cell lines T47DshER-α and MDA-MB-231pEGFPC1-ER-α cells (See Figure S2F for generation of stable cell line). As anticipated loss of functional ER-α delayed DSB repair in T47DshER-α cells with long term persistence of γH2AX foci (**Figure 3D**, Quantification below), on the contrary introduction of wild-type ER-α in MDA-MB-231 cells (MDA-MB-231pEGFP C1-ER-α) rescued the cells from cisplatin induced DNA-DSB with timely nuclear recruitment and gradual decline in γH2AX foci within 48 hours of repair time (**Figure 3E**, Quantification below).

Wild type BRCA1 or p53 did not rescue ER-α deficient breast cancer cells from DNA-DSB

BRCA1 is a cardinal player of DNA-DSB repair. However, the knockdown of BRCA1 in MDA-MB-231 cells did not affect its γH2AX kinetics compared to its wild-type controls. Thus, we analyzed whether introduction of wild type BRCA1, in ER-α negative BRCA1 mutant cells,

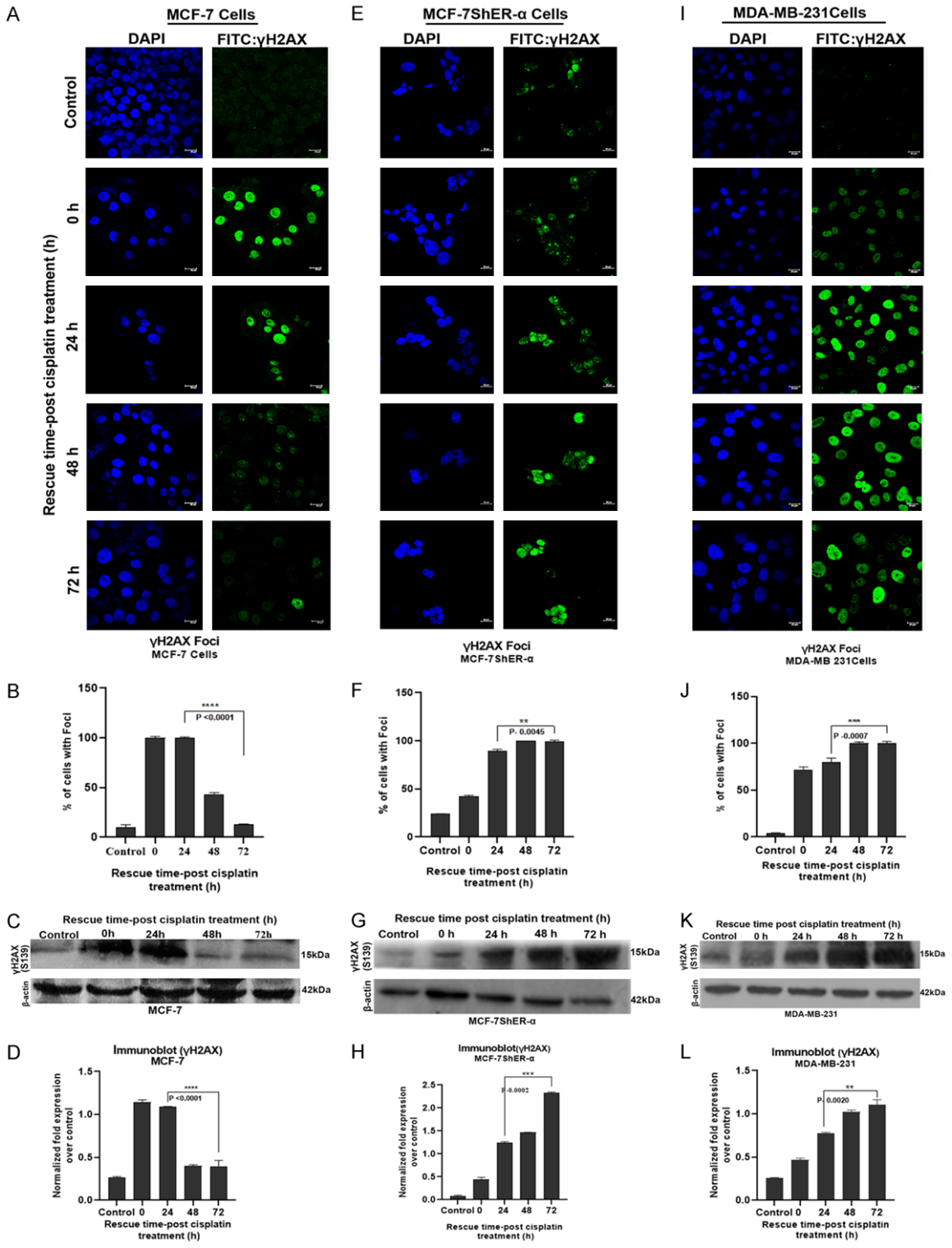

Figure 2. Cisplatin induced DNA-DSB results in persistent induction of γH2AX expression and activation of DDR in ER-α deficient cells. (A, B) Immmunoflurescence staining of γH2AX scored at different time points post cisplatin induced DSB. (C, D) western blot analysis for expression of γH2AX upon 5 μM cisplatin induced DNA DSB and post treatment rescue in MCF-7 cells. (E-H) Comparable data, respectively in MCF-7shER-α cells and (I-L) in MDA-MB-231 cells. Experiment was repeated thrice and the percentage of foci positive cells were counted manually, 10 microscopic fields with not less than 10 cells were counted for each sample (40X, Scale bar 20 μm), (Error bars, mean ± SD, $^{*}P\leq0.05$ and $^{**}P\leq0.005$ and as $^{***}P\leq0.001$, $^{****}P\leq0.0001$ unpaired t-test). (The extra nuclear DAPI observed with **Figure 2A** could be an over exposure or over loaded DAPI, which is usually observed with the use of DAPI containing mounting media).

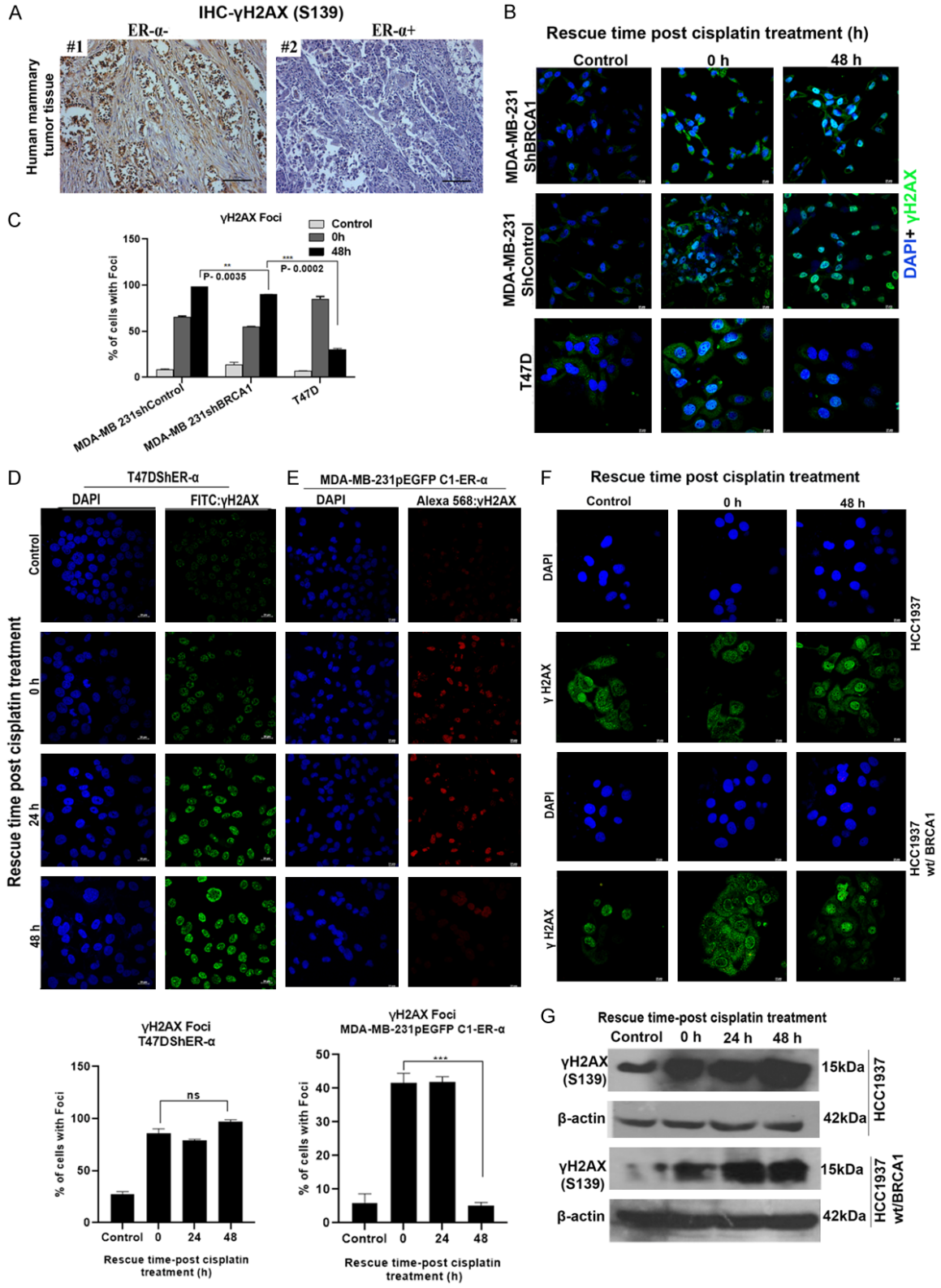

Figure 3. "Wild type BRCA1 or p53 did not rescue of ER-α deficient breast cancer cells from DNA-DSB". (A) Representative image for IHC staining for γH2AX in treatment naive, ER-α$^+$ and ER-α$^-$ human breast tumor tissues (20X, Scale bar 100 μm, ER-α$^+$/ER-α$^-$ tumor n=4). (B, C) Immmunofluorescence staining of γH2AX and % of foci positive cells upon 5 μM cisplatin induced DNA-DSB and post treatment rescue respectively in MDA-MB-231shBRCA1 and T47D cells. (D, E) Immmunofluorescence staining of γH2AX and % of foci positive cells (quantification-below) upon 5

μM cisplatin induced DNA-DSB and post treatment rescue respectively in T47DshER-α and MDA-MB-231pEGFP C1-ER-α cells, scored at different time points of rescue. (F) Immmunofluorescence staining and (G) Western blot analysis for the expression of γH2AX in response to cisplatin induced DNA-DSB and post treatment rescue, respectively in HCC1937 and HCC1937 wt/BRCA1. ((A) scale bar-100 μm. (B-F) scale bar-20, 10 μm, 60X). (Error bars, mean ± SD, $^{*}P\leq0.05$ and $^{**}P\leq0.005$ and as $^{***}P\leq0.001$, $^{****}P\leq0.0001$, unpaired t-test). Alexa 568 is used as fluorochrome for immmunofluorescence in GFP expressing cells.

can re-activate their DNA-DSB repair efficiency. We scored the γH2AX kinetics of triple negative, BRCA1-mutated human breast cancer cell line, *HCC1937,* and its genetically identical clone, HCC1937 wt/BRCA1 which has a high expression of wild-type BRCA1, after induction of DNA-DSB (**Figure 3F**, **3G**). Both the cell lines gave similar results with aberrant γH2AX kinetics and persistent activation of γH2AX foci even after 48 hours of rescue. Even though the γH2AX kinetics was similar; the endogenous expression of γH2AX was higher in BRCA1 mutant HCC1937 cells. These results indicate that though the presence of wild type BRCA1 is critical for DSB repair, it could not activate the delayed damage repair ability in ER-α negative cells even up to 48 hours. This signifies that besides BRCA1, ER-α might also have a fundamental role to play in DNA-DSB repair.

However, the cell lines used for the study MCF-7 (p53 wild-type), MDA-MB-231, T47D and HCC1937 (p53 mutant) have different genetic background and p53 statuses. Thus, to rule out the possible effect of p53 in DSB repair and to eliminate or understand the effects of p53 in DNA damage response/repair, we stably overexpressed wild-type p53 in p53 mutant MDA-MB-231 and T47D cells (See Figure S2F for generation of stable cell line). Next we analyzed the ability of these cells to repair cisplatin induced DNA-DSB by scoring of γH2AX kinetics. It was observed that even with the introduction of wild-type p53 the cells could not rescue from the DSB-damage and modulate the repair kinetics, in comparison to their respective control cells (**Figure 4A**), thereby indicating that the delayed DDR elicited by ER-α efficient cells was not attributable to p53 mutation.

Henceforth, though it is reported that ER-α represses p53, in certain conditions, it can also up-regulate p53, but sequester it without completely affecting its sentinel role in regulating cellular proliferation and apoptosis [25, 26]. Thus, the interplay between p53, ER-α and BRCA1 in DDR is yet to be identified and might require further experimental validations.

Ligand-dependent ER-α transactivation influences the DDR in breast cancer cells

Since ER-α deficient breast cancer cells could not recover from the exogenously induced DSB over time, we analyzed the molecular mechanism of this feature by assessing the effect of estrogen. For this, we generated an *in vitro* system by growing the E2 responsive cells in E2 deprived condition, which would closely mimic the clinical conditions of estrogen deprivation as in salpingo oophorectomy or other primary endocrine therapy. During this estrogen deprivation, the un-liganded estrogen-receptors might bind to their respective response elements (ERE) and initiate transcription allowing the cells to adapt and re-grow [27].

We could observe that E2 responsive MCF-7 cells survived the estrogen deprivation, adapted themselves and showed re-growth with a gradual increase in ER-α expression both at mRNA and at protein levels, when analyzed at 10 days interval for 50 days (Figure S2G, S2H).

Further, we scored the γH2AX kinetics of these cells (grown in E2 deprivation conditions) in response to cisplatin-induced DNA-DSB. γH2AX foci peaked at 24 hours-post cisplatin treatment and persisted in the nuclei with longer rescue time, indicative of impeded DDR and repair. However, when these cells were activated by re-introduction of 10 nM 17-β Estradiol, the γH2AX foci disappeared gradually; which was similar to the result observed with wild-type MCF-7 cells during DNA-DSB repair (**Figure 4B-E**), indicating that like ER-α deficiency, reduced E2 levels can also affect DDR in cells. Briefly, ER-α^{+} cells grown in estrogen deprivation exhibited increased ER-α expression. However, in response to DSB they elicited persistent γH2AX activation similar to ER-α deficient cells. This implies that deficiency of either the ligand (E2), the receptor (ER-α) or both would alter DDR in cells.

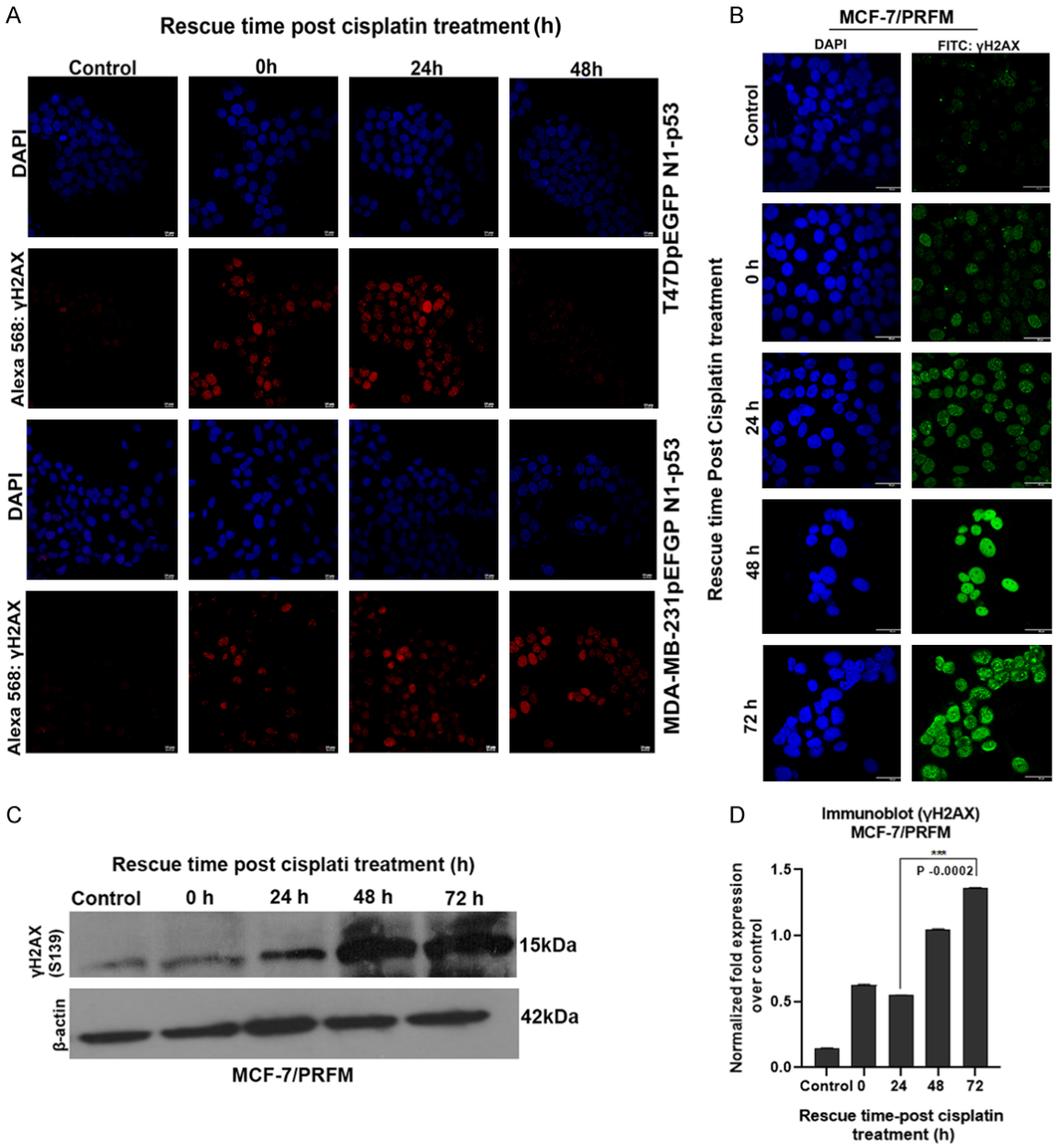
A
Rescue time post cisplatin treatment (h)
Control
0h
24h
48h
DAPI
Alexa 568: γH2AX
T47DpEGFP N1-p53
DAPI
Alexa 568: γH2AX
MDA-MB-231pEFGP N1-p53
B
MCF-7/PRFM
DAPI
FITC: γH2AX
Control
0 h
24 h
48 h
72 h
Rescue time Post Cisplatin treatment
C
Rescue time post cisplati treatment (h)
Control
0 h
24 h
48 h
72 h
γH2AX (S139)
β-actin
15kDa
42kDa
MCF-7/PRFM
D
Immunoblot (γH2AX)
MCF-7/PRFM
***
P -0.0002
Normalized fold expression over control
1.5
1.0
0.5
0.0
Control 0
24
48
72
Rescue time-post cisplatin treatment (h)
E
Rescue time post cisplatin treatment (h)
0h
72h
PRFM
PRFM+10nM 17-β estradiol
DAPI+γH2AX
F
Rescue time post cisplatin treatment (h)
Control
0 h
48 h
MCF-7/pcDNA3ER-α
MCF-7+ 5μM tamoxifen
DAPI+γH2AX

Figure 4. Deregulated E2-ER delays DDR in estrogen responsive cells. (A) Immmunofluorescence staining of γH2AX upon 5 μM cisplatin induced DNA-DSB and post treatment rescue respectively in p53 over-expressing, T47DpEGFP N1-p53 and MDA-MB-231 pEGFP N1-p53 cells scored at different time points of rescue. (B) The immmunofluorescence staining and (C, D) western blot analysis of γH2AX post DSB induction, in MCF-7 cells grown in E2 deprivation (MCF-7/PRFM), the deregulation of E2-ER-α in these cells delayed DDR and retained damage response foci beyond 48 hours of rescue, but with reactivation using E2 (10 nM 17-β Estradiol) (E) cells regained DDR ability. (60X, Scale bar 20 μm). (F) Immmunofluorescence staining for γH2AX, in MCF-7pCDNA3ER-α and 5 μM (12 hours) tamoxifen citrate treated MCF-7 cells. Tamoxifen citrate treated MCF-7 cells retained damage response foci 48 h post cisplatin treatment. (Error bars, mean ± SD, *P≤0.05 and **P≤0.005 and as ***P≤0.001, ****P≤0.0001, unpaired t-test).

To mimic the ER-α over expression observed with E2 deprivation, we stably over-expressed ER-α in wild type MCF-7 cells (MCF-7pcDNA3ER-α cells -see Figure S2I-K for ER-α over expression) and replicated the experiment in MCF-7pcDNA3ER-α cells. In contrast to cells grown in E2 deprivation or ER-α deficient cells, these cells repaired the DNA-DSB in 48 hours of rescue with gradual decrease in γH2AX expression (**Figure 4F**, top panel). Concurrently, we inhibited functional ER-α in MCF-7 cells by treating the cells with 5 μM tamoxifen citrate (Inhibitor of ER-α activity) for 12 hours. In tamoxifen treated MCF-7 cells, the γH2AX foci persisted beyond 48 hours of rescue and showed a delayed damage repair (**Figure 4F**, bottom panel). Thus any abrogation in ER-α activity arising as a result of either E2 (ligand) or ER-α (receptor) deficiency would delay DDR in cells without significantly affecting the cell proliferation. Thus, we strongly believe that pharmacological inhibition of ER-α signaling might have clinical implications, as it could impact BRCA1-mediated DNA repair activities in the cells, further leading to accumulation of unrepaired damages.

These results, collectively indicates that rather than the expression of ER-α, an active ligand-dependent ER-α transactivation is a requisite for augmenting DNA-DSB repair in breast cancer cells.

Ligand-dependent ER-α transactivation modulates nuclear recruitment of major DDR proteins

As ER-α deficient cells exhibited delayed damage repair with persistent activation of γH2AX, we further analyzed the expression and kinetics of downstream DDR regulators. γH2AX is one of the early damage sensing proteins recruited to the site of DNA-DSB that further initiates the sequential recruitment of downstream effectors.

Localization of phosphorylated BRCA1 to the nuclear damage site and its de-phosphoryation on repair of DNA damage is a critical event in DDR. Among other phosphorylation events, BRCA1, S^{988} phosphorylation (pS988-BRCA1) is specific to trigger DSB repair particularly through the HRR. The BRCA1 phosphorylations, pS1524-BRCA1 and pS1423-BRCA1 are reported to function in other biological process like caspase activation, whereas pS988-BRCA1 is specific to trigger HRR. Thus, kinetics of pS988-BRCA1, in response to cisplatin induced DSB was analyzed by ICC. In MCF-7 cells, pS988-BRCA1 was recruited to the nuclear damage site and was gradually declining with post treatment rescue. On the contrary, ER-α deficient MCF-7shER-α cells, MDA-MB-231 cells as well as cells grown in E2 deprived media, exhibited reduced pS988-BRCA1 expression and localization, with delayed nuclear recruitment and persistence of foci beyond 48 hours of rescue. Moreover, MCF-7shER-α as well as MDA-MB-231 cells exhibited visible damage response foci even in untreated controls indicative of their increased damage sensitivity in the absence of ER-α (**Figure 5A**, **5B**). However, we could not observe any significant difference in expression or nuclear recruitment of pS1524-BRCA1 and pS1423-BRCA1, in ER-α proficient or deficient cells post cisplatin treatment as analyzed by ICC (Figure S3A), indicating that decreased ER-α activity predominantly affects HRR in cells.

pS988-BRCA1 and 53BP1 are reported to have decisive role in DSB repair pathway; while pS988-BRCA1 facilitates DSB repair through HRR, 53BP1 activation promotes NHEJ [28]. Thus, we also analyzed the expression of 53BP1 in response to cisplatin induced DNA-DSB. MCF-7 cells exhibited significantly higher expression of 53BP1, in comparison with ER-α^{-} cells; whereas both the cell lines elicited similar expression kinetics of 53BP1 in response to DNA-DSB (**Figure 5C**).

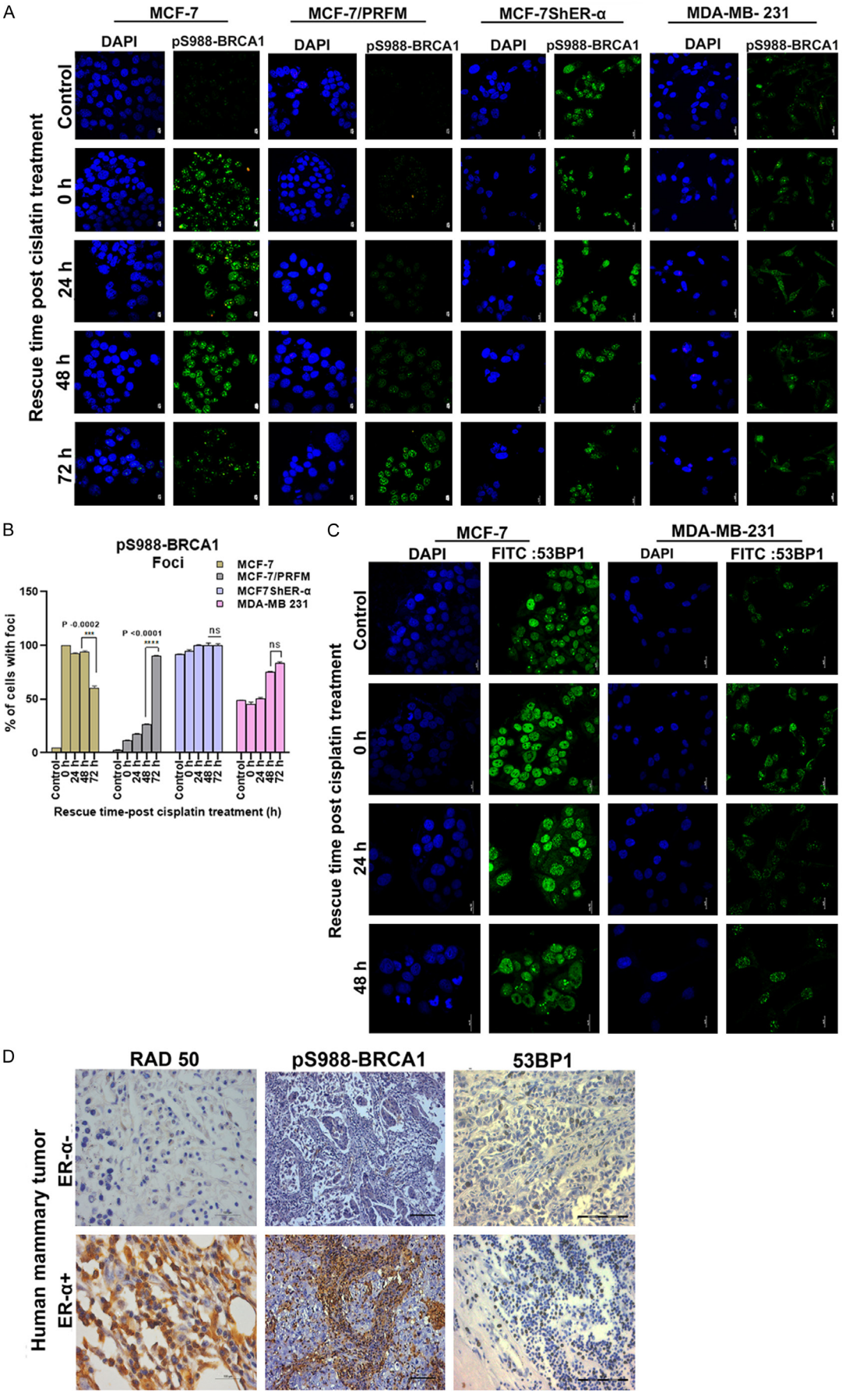
A
MCF-7
MCF-7/PRFM
MCF-7ShER-α
MDA-MB- 231
DAPI
pS988-BRCA1
Control
0 h
24 h
48 h
72 h
Rescue time post cislatin treatment
B
pS988-BRCA1
Foci
MCF-7
MCF-7/PRFM
MCF7ShER-α
MDA-MB 231
% of cells with foci
P -0.0002
P <0.0001
ns
Rescue time-post cisplatin treatment (h)
C
MCF-7
MDA-MB-231
DAPI
FITC :53BP1
Rescue time post cisplatin treatment
D
RAD 50
pS988-BRCA1
53BP1
Human mammary tumor
ER-α-
ER-α+

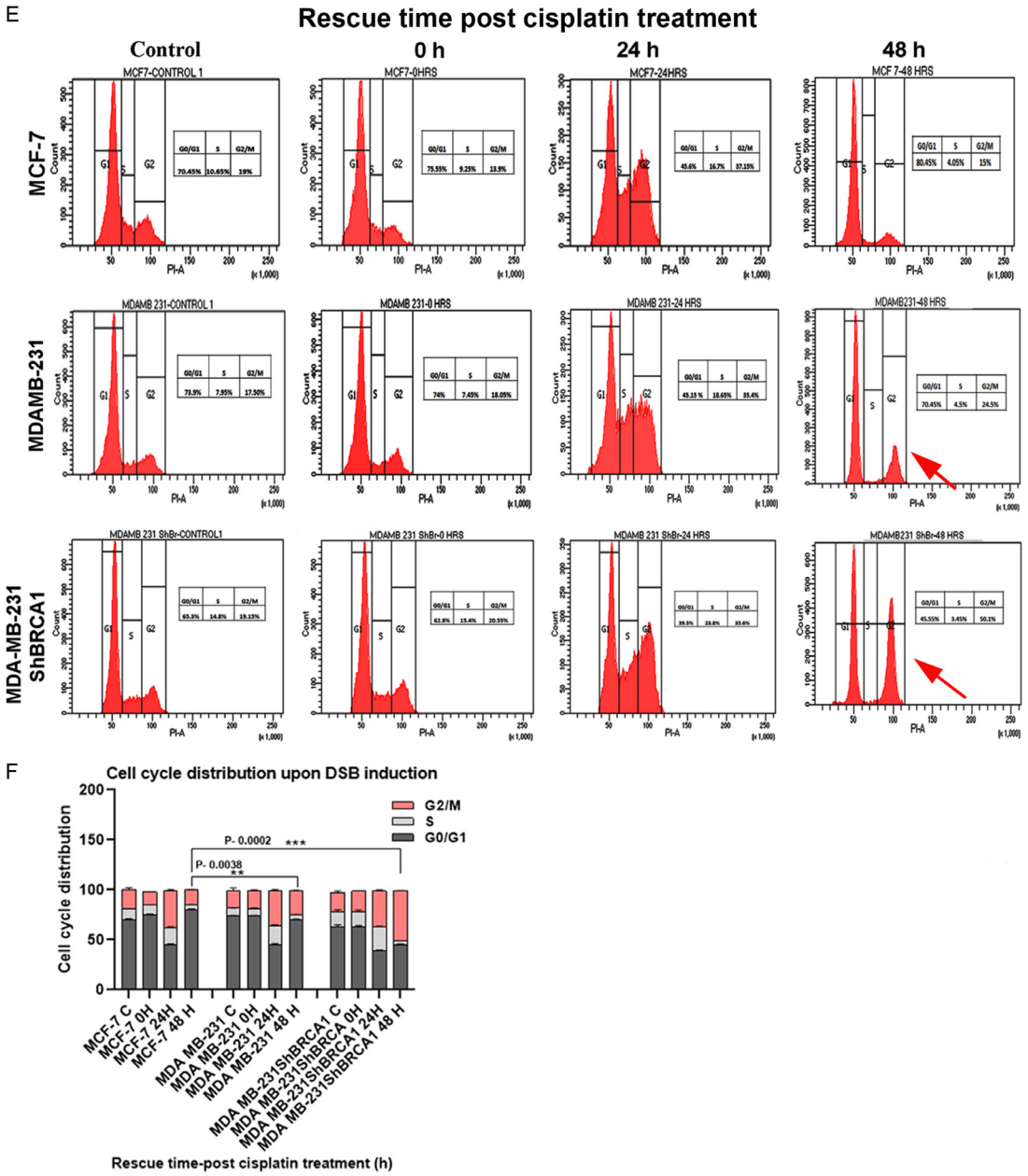

Figure 5. ER-α deficiency impedes nuclear recruitment of major DDR proteins. (A, B) Immmunofluorescence staining, for phosphorylated-BRCA1-S988 (pS988-BRCA1) formed in response to 5 μM cisplatin induced DNA-DSB, respectively in MCF-7, MCF-7/PRFM, MCF-7shER-α and MDA-MB-231 cell lines. The percentage of foci positive cells was counted manually, 10 microscopic fields with not less than 10 cells were counted for each sample. (60X, Scale bar 20 μm). (C) 5 μM cisplatin induced damage response foci of 53BP1, in MCF-7 and MDA-MB-231 cells analyzed by Immmunofluorescence staining (60X, Scale bar 20 μm). (D) IHC staining for major DDR proteins RAD50, pS988-BRCA1 and 53BP1 respectively in ER-α$^+$ and ER-α$^-$ treatment naive human breast tumor tissues (20X, Scale bar 100 μm, ER-α$^+$/ER-α$^-$ tissue, n=4). (E, F) ER-α knock down impedes G2/M checkpoint recovery and cell cycle progression in DSB induced breast cancer cells. (E) Cell cycle distribution and (F) quantification, in DNA-DSB induced MCF-7, MDA-MB-231 and MDA-MB-231shBRCA1 cells, scored at different time points of post treatment rescue. (Error bars, mean ± SD, *P≤0.05 and **P≤0.005 and as ***P≤0.001, ****P≤0.0001, unpaired t-test).

Concurrently, the expression of key HRR regulator complex, MRN (MRE11, RAD50 and NBS1), were significantly reduced in ER-α$^-$ cells with respect to ER-α$^+$ cells. Nuclear localization and considerably higher expression of MRE11 and RAD50 were observed in MCF-7 cells in comparison with MDA-MB-231 cells upon DNA-DSB repair (Figure S3B). We also observed a higher

expression and localization of HRR regulators; pS988-BRCA1 and RAD50, in ER-α^+ human breast tumor tissues in comparison with ER-α^- ones as analyzed by IHC. However, there was no significant difference in the expression of the NHEJ regulator 53BP1 between the tissues (**Figure 5D**).

Thus, in ER-α^- cells, there was aberrant expression of p-BRCA1/MRE11 and RAD50 as well as persistent expression of 53BP1 foci in response to DSB. These signify that it is not HRR but NHEJ is the inherent and active pathway of DNA-DSB repair in ER-α deficient cells. Conversely the active ER-α signaling in ER-α^+ cells promote HRR over NHEJ. (53BP1 expression observed in ER-α^+ MCF-7 cells need not be confounded, as we have used asynchronously proliferating cells and NHEJ is identified to be active throughout the cell cycle [29]).

ER-α regulate G2/M arrest and re-entry of cells into cell cycle

Altered expression of 53BP1 and pS988-BRCA1 is reported to influence the cell cycle progression [28, 30]. DNA-DSBs are repaired at G2/M phase allowing the recovered cells to enter the next phase of cell cycle. Therefore, we next analyzed the cell-cycle progression in exponentially growing (asynchronous) breast cancer cells following induction of DSBs.

To see whether ER-α can regulate DNA repair at G2/M phase, the cell cycle distribution in MCF-7, MDA-MB-231 and MDA-MB-231shBRCA1 cells in response to DNA-DSB was analyzed by flow cytometry. It was observed that at 24 hours of rescue, all treated cells were retained in G2-M phase. However, after 48 hours of rescue, in comparison to MDA-MB-231 and MDA-MB-231shBRCA1 cells, significantly higher percentage of MCF-7 cells progressed to next phase (G1) of cell cycle. A large population of MDA-MB-231 and MDA-MB-231shBRCA1 cells was restrained at the G2-M phase, indicative of their impaired or delayed repair efficiency (**Figure 5E**, **5F**). These results indicated that the absence of either ER-α or BRCA1 would adversely affect the repair pathways in cells. However, the loss of BRCA1 along with deregulation of ER-α signaling together would greatly impact the DDR in estrogen responsive cells resulting in genomic instability.

These ER-α deficient cells elicited a delayed repair or partially repaired DSBs at G2-M checkpoint and as a consequence exhibited significantly higher amount of chromosome defects such as breaks and fragmented DNA as analyzed by neutral comet assay and metaphase chromosome spreads (Figure S3C, S3D). Hence, it is evident that as reported with BRCA1 defective conditions, ER-α deficiency can also lead to delayed G2/M progression, an indication of defective DSB repair.

ER-α deficiency limits BRCA1 mediated HRR and promote DSB repair through NHEJ in breast cancer cells

As we observed delayed DSB repair, decreased expression and aberrant nuclear recruitment of HRR proteins in ER-α^- cells, we next evaluated the cells for their HR efficiency. To evaluate the HR efficiency, a plasmid based *in vitro* HR assay was used (Figure S4A). As anticipated, the HR efficiency was significantly reduced in BRCA1 knockdown MCF-7shBRCA1 and MDA-MB-231shBRCA1 cells in comparison to their corresponding controls. However, it was observed that ER-α deficient MCF-7shER-α and MDA-MB-231 cells also showed reduced HR efficiency when compared to control cells (**Figure 6A-F**). In addition, estrogen deprivation significantly reduced the HRR in MCF-7 cells, however; the cells regained its HR efficiency when supplemented with 10^{-8} M 17-β estradiol (**Figure 6G**, **6H**). Consistently, treatment with tamoxifen citrate considerably reduced the HR efficiency in MCF-7 cells (**Figure 6I**, **6J**). This implies that the reduced estrogen and ER-α activity can alter BRCA1 mediated HRR in estrogen responsive cells.

The above results were further confirmed using an HR-NHEJ construct DR-GFP [31, 32], which facilitates the precise scoring of NHEJ: HR ratio in the cells (Figure S4B). MCF-7, MCF-7shER-α, MCF-7pcDNA3ER-α and MDA-MB-231 cells stably expressing DR-GFP were generated through transfections and site specific DSB were created in these cells using I-Sce coding plasmids. Upon I-Sce-induced DSB and follow on incubation, the HRR efficient cells express GFP. The backbone vectors pgkPURO and pCAGGSS-mCherry (#41583, addgene) were respectively used for mock transfections.

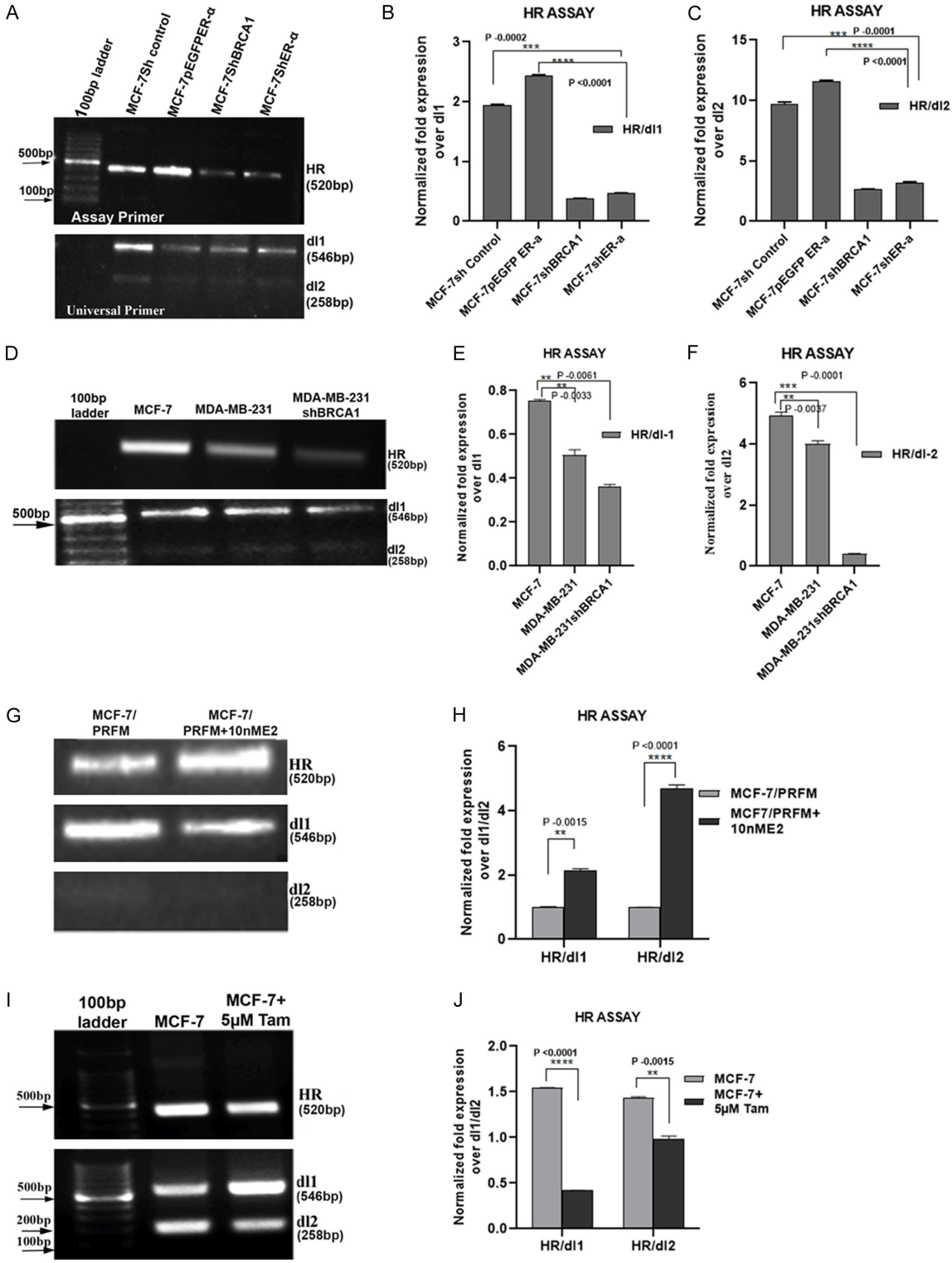
A
100bp ladder
MCF-7Sh control
MCF-7pEGFPER-α
MCF-7ShBRCA1
MCF-7ShER-α
500bp
100bp
HR (520bp)
Assay Primer
dl1 (546bp)
dl2 (258bp)
Universal Primer
B
HR ASSAY
Normalized fold expression over dl1
P -0.0002
***
****
P <0.0001
HR/dl1
MCF-7sh Control
MCF-7pEGFP ER-a
MCF-7shBRCA1
MCF-7shER-a
C
HR ASSAY
Normalized fold expression over dl2
*** P -0.0001
****
P <0.0001
HR/dl2
D
100bp ladder
MCF-7
MDA-MB-231
MDA-MB-231 shBRCA1
HR (520bp)
500bp
dl1 (546bp)
dl2 (258bp)
E
HR ASSAY
Normalized fold expression over dl1
** P -0.0061
**
P -0.0033
HR/dl-1
MCF-7
MDA-MB-231
MDA-MB-231shBRCA1
F
HR ASSAY
Normalized fold expression over dl2
P -0.0001
***
**
P -0.0037
HR/dl-2
G
MCF-7/ PRFM
MCF-7/ PRFM+10nME2
HR (520bp)
dl1 (546bp)
dl2 (258bp)
H
HR ASSAY
Normalized fold expression over dl1/dl2
P -0.0015
**
P <0.0001
****
MCF-7/PRFM
MCF7/PRFM+ 10nME2
HR/dl1
HR/dl2
I
100bp ladder
MCF-7
MCF-7+ 5μM Tam
500bp
HR (520bp)
500bp
dl1 (546bp)
200bp
dl2 (258bp)
100bp
J
HR ASSAY
Normalized fold expression over dl1/dl2
P <0.0001
****
P -0.0015
**
MCF-7
MCF-7+ 5μM Tam
HR/dl1
HR/dl2

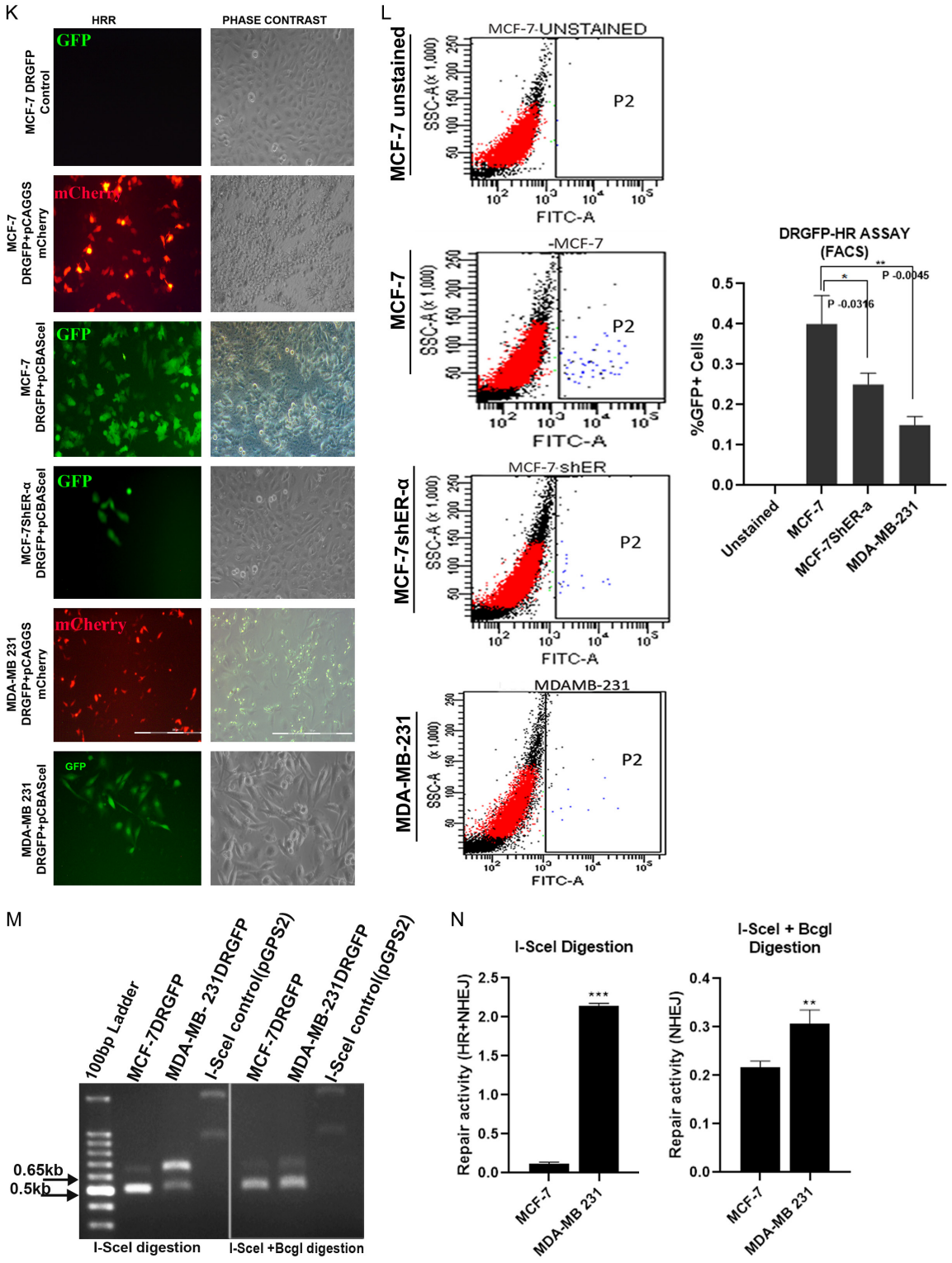

Figure 6. ER-α deficiency impairs BRCA1 mediated HRR and promote NHEJ. (A) Homologous recombination efficiency of MCF-7, MCF-7ShER-α, MCF-7ShBRCA1 and MCF-pEGFP ER-α cells, as analyzed by HR assay; (B, C) HR product formed upon recombination is quantified and normalized with respective backbone plasmids dI1 and dI2. (D) Homologous recombination efficiency of MDA-MB-231 and MDA-MB-231shBRCA1 cells as analyzed by HR assay, (E, F) normalized to backbone plasmids dI1 and dI2. (G, H) Homologous recombination efficiency of MCF-7 cells analyzed post estrogen deprivation and follow on activation using 17-β estradiol. (I, J) MCF-7 cells were treated with 5 μM Tamoxifen citrate for 12 hours to inhibit ER-α activity and HR efficiency was further scored using HR as-

say. (K-N) DRGFP based HR assay: MCF-7, MCF-ShER-α, and MDA-MB-231 cells stably expressing pDR-GFP, were transfected with I-SceI expression vector (pCBASceI) or mock (pCAGGS-mCherry) to generate a DSB within the Sce-GFP. (K) Immmunofluorescence and (L) Fluorescence-activated cell sorting (FACS) analysis carried out to quantify HR-repaired GFP+ cells. ER-α expressing cells generated higher percentage of GFP+ cells. Each value represents the mean ± SD of three independent experiments. For assessing NHEJ activity, DR-GFP-integrated MCF-7 and MDA-MB-231 cells were transfected with mock or I-SceI and 48 hours post transfection, genomic DNA was extracted for PCR amplification (Figure S5A), followed by I-SceI or I-SceI plus BcgI digestion, and the digested products were subjected to gel electrophoresis (M). Since HR repair will replace the I-SceI site with the BcgI site and the NHEJ repair will diminish both the enzyme sites, the ratio between uncut DNA and cut DNA after I-SceI digestion represents "HR + NHEJ repair" efficiency while this ratio between uncut DNA and cut DNA after I-SceI and BcgI digestion reflects only the NHEJ repair efficiency (N). (See Figure S4B for detailed protocol) (Error bars, mean ± SD, *P≤0.05 and **P≤0.005 and as ***P≤0.001, ****P≤0.0001, unpaired t-test).

The GFP^{+} cells arising as a result of HRR, were significantly higher in MCF-7 cells in comparison with the MCF-7shER-α and MDA-MB-231 cells, as analyzed by fluorescent microscopy and flow cytometry (Fluorescent intensities and transfection efficiency of the cells were normalized with control/mock transfected cells) (**Figure 6K**, **6L**). There was higher HR activity and concurrent GFP expression in ER-α positive cells in comparison to ER-α negative cells.

It was also observed that a significantly higher percentage of ER-α^{+} MCF-7 cells recovered I-Sce induced DSB, and thus elicited higher colonigenic potential, in comparison with the ER-α knockdown cells, as analyzed by CFA (Figure S4C, S4D). This implies that the damage repair and rescue capacity is higher in presence of functional ER-α. To rule out the possibility that the reduced colonigenic ability exhibited by MCF-7shER-α cells was not directly due to ER-α knockdown and is correlated with the reduced HRR and delayed damage rescue, we further analyzed the expression of proliferation markers. Corroborating the above results, proliferation markers PCNA and Ki67 did not show significant differences between MCF-7, MCF-7pcDNA3ER-α, MCF-7pEGFPER-α and MCF-7shER-α cells (Figure S4E, S4F). The colony forming ability of MCF-7 and MCF-7shER-α also did not significantly differ from each other (Figure S4G, S4H), substantiating that the ER-α knock down cells did not affect proliferation ability of MCF-7 cells.

Since DDR events are cell cycle dependent and as we have used asynchronously proliferating cells for the study, it is also obligatory to analyze the second major pathway of DSB repair, NHEJ. For analyzing NHEJ/HR ratio or NHEJ activity alone, the genomic DNA was extracted from the cells after I-Sce transfection, amplified using specific primers and exposed to restriction digestion. Compared to ER-α^{+} cells, HR efficiency was significantly reduced in ER-α^{-} cells, though, these cells showed increased NHEJ activity (Figures S5A, **6M** and **6N**).

The above results were validated with cell free *in vitro* NHEJ assay, using nuclear extracts from DSB induced cells. Wild-type MCF-7 cells showed significantly lower end-joining activity in comparison with ER-α deficient MDA-MB-231 and MCF-7shER-α cells (**Figure 7A**, **7B**).

Observing the higher rate of NHEJ in ER-α deficient cells, we further analyzed the expression of NHEJ regulator DNA-PK in MCF-7, MDA-MB-231 and MDA-MB-231shBRCA1 cells in response to DSB. There was no significant difference in the DNA-PK mRNA expression between the cells; however, the MDA-MB-231 (ER-α deficient) and MDA-MB-231shBRCA1 (ER-α and BRCA1 deficient) cells elicited higher expression of DNA-PK protein (Figure S5B, S5C).

The expression of major NHEJ proteins KU80 and DNA-PK was significantly higher in ER-α^{-} human tumor tissues as well, when compared to the ER-α^{+} tissues as analyzed by IHC. This might be an indication of an active NHEJ against persisting damages in ER-α deficient condition (**Figure 7C**). We next inhibited NHEJ pathway in the cells, with a ligase IV-NHEJ inhibitor-SCR-Pyrazine. In MCF-7 cells this treatment resulted in significantly higher protein/mRNA expression of ER-α as well as BRCA1 in response to DSB (**Figure 7D-F**). However, the ER-α deficient cells did not show any significant difference in their BRCA1 levels, in response to damage even with an impediment in NHEJ pathway (**Figure 7G**, **7H**). Thus, even with an inhibition in the NHEJ pathway the ER-α deficient cells could not activate BRCA1 and trigger

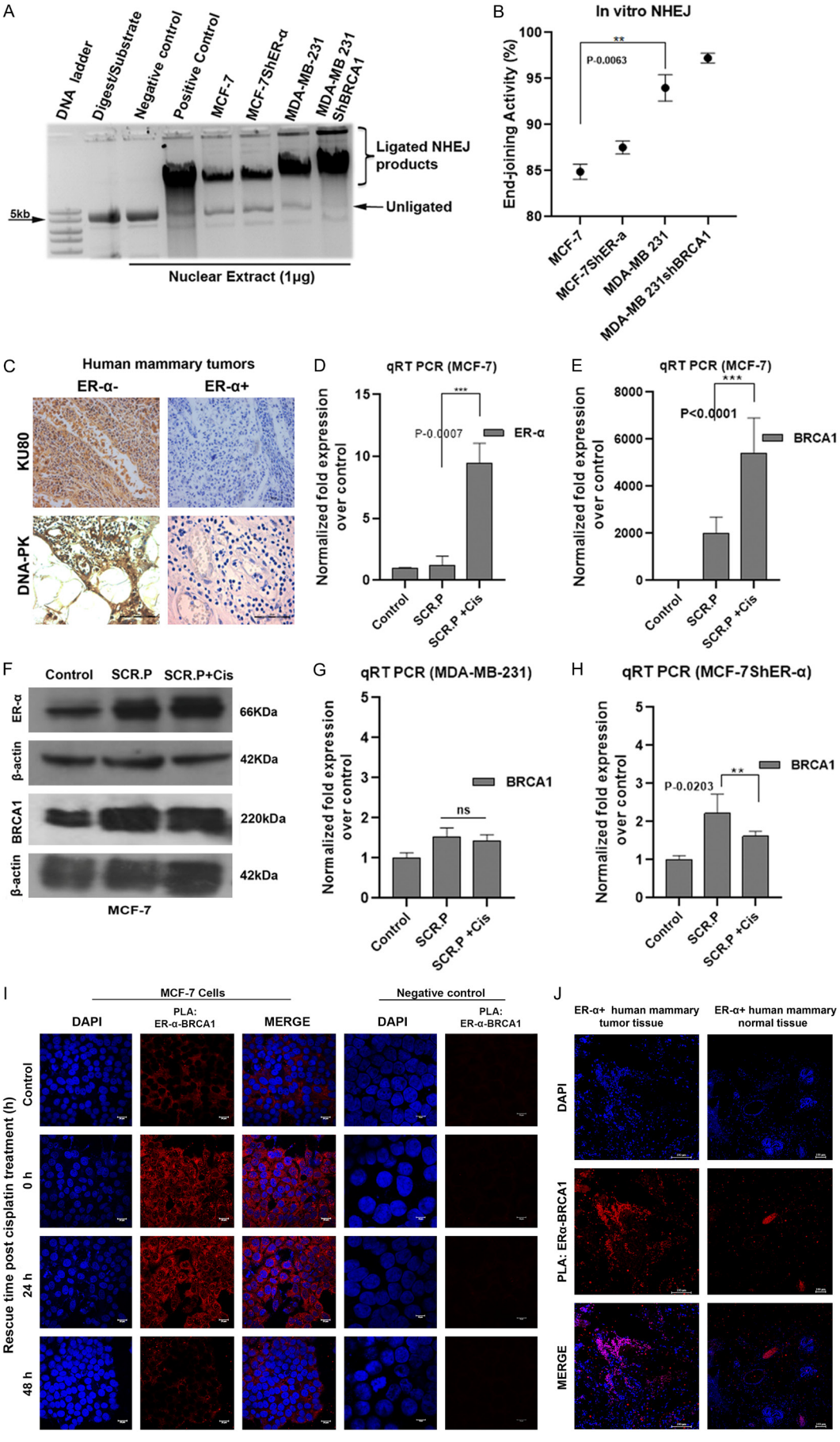
A
DNA ladder
Digest/Substrate
Negative control
Positive Control
MCF-7
MCF-7ShER-α
MDA-MB-231
MDA-MB 231 ShBRCA1
Ligated NHEJ products
Unligated
5kb
Nuclear Extract (1µg)
B
In vitro NHEJ
End-joining Activity (%)
P-0.0063
MCF-7
MCF-7ShER-a
MDA-MB 231
MDA-MB 231shBRCA1
C
Human mammary tumors
ER-α-
ER-α+
KU80
DNA-PK
D
qRT PCR (MCF-7)
Normalized fold expression over control
P-0.0007
ER-α
Control
SCR.P
SCR.P +Cis
E
qRT PCR (MCF-7)
P<0.0001
BRCA1
F
Control
SCR.P
SCR.P+Cis
ER-α
β-actin
BRCA1
66KDa
42KDa
220kDa
MCF-7
G
qRT PCR (MDA-MB-231)
ns
H
qRT PCR (MCF-7ShER-α)
P-0.0203
I
MCF-7 Cells
Negative control
DAPI
PLA: ER-α-BRCA1
MERGE
Rescue time post cisplatin treatment (h)
Control
0 h
24 h
48 h
J
ER-α+ human mammary tumor tissue
ER-α+ human mammary normal tissue
PLA: ERα-BRCA1

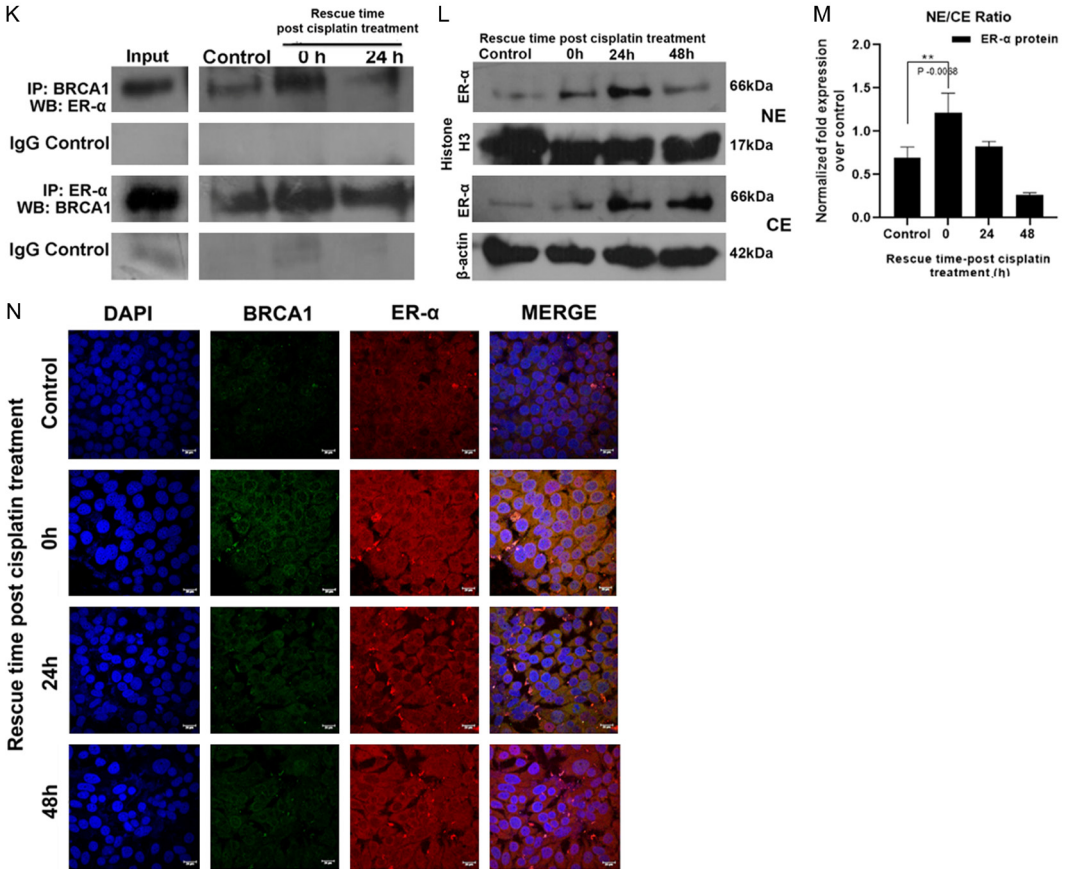

Figure 7. ER-α deficiency promote NHEJ. Linearized plasmid substrates with cohesive ends were generated by EcoRI restriction digestion. 250 ng of the purified linearized plasmid substrate was incubated with 1 μg of nuclear protein extracts from DSB induced MCF-7, MCF-7shER-α, MDA-MB 231, MDA-MB 231shBRCA1 cells in the end joining reaction buffer. NHEJ products formed were separated on agarose gel and the band intensities were normalized to substrate bands, substrate incubated with nuclear lysate from those cells treated with NHEJ-Ligase IV inhibitor SCR-Pyrazine, was used as negative control. (A, B) Represents the end joining activity in different cell lines. (C) IHC staining of KU80 and DNA-PK in ER-α^{+} and ER-α^{-} treatment naive human breast tumor tissues (20X, Scale bar 100 μm, ER-α^{+}/ER-α^{-} tissue n=4). (D, E) qRT-PCR and (F) western blot analysis for the expression of ER-α and BRCA1 in MCF-7 cells, treated with 30 μM SCR-pyrazine (SCR.P) a ligase IV-NHEJ inhibitor for 24 hours, prior to induction of DNA DSB using 5 μM cisplatin. (G, H) Represents the mRNA expression of BRCA1 in response to cisplatin induced DSB, in SCR pyrazine treated MDA-MB-231 and MCF7shER-α cells. (Error bars, mean ± SD, *P≤0.05 and **P≤0.005 and as ***P≤0.001, ****P≤0.0001, unpaired t-test). DNA-DSB repair entails a protein-protein interaction between BRCA1 and ER-α. (I) The protein-protein interaction between ER-α and BRCA1 (Red Fluorescent spots) in MCF-7 cells upon cisplatin induced DSB and follow on rescue as analyzed by PLA (60X, Scale bar 10 μm). PLA with MDA-MB-231, an ER-α deficient cell line, was used as a negative control (ER-α Vs BRCA1). (J) Treatment naive ER-α^{+} human breast tumor FFPE sections showing protein-protein interaction between BRCA1 and ER-α, as analyzed by PLA. Adjacent normal section from the same patient served as the control (10X, Scale bar 100 μm). (K) Co-immuno-precipitation (IP-BRCA1, WB: ER-α and IP-ER-α, WB: BRCA1) showing protein-protein interaction between ER-α and BRCA1 in response to DNA-DSB in 5 μM cisplatin treated MCF-7 cells. (L) Western blot analysis and (M) nuclear to cytoplasmic ratio/expression of ER-α protein in response to cisplatin induced DNA-DSB, in MCF-7 cells, analyzed at different time points post cisplatin treatment. (NE and CE respectively represent nuclear extract and cytoplasmic extract. Band intensities are respectively normalized to Histone H3 and β-actin). (Error bars, mean ± SD, *P≤0.05 and **P≤0.005 and as ***P≤0.001, ****P≤0.0001-unpaired t-test). (N) Immmunofluorescence image showing the co-localization of ER-α and BRCA1 in DNA-DSB induced MCF-7 cells analyzed at different time points of rescue (60X, Scale bar 20 μm).

HRR. Collectively, these results indicate that, presence of a functional ER-α might augment BRCA1 and its repair activity. Whereas, ER-α deficiency or defects in E2-ER (Estrogen-Estrogen receptor) signaling might reduce the HRR in cells facilitating the DSB repair through low-fidelity repairs like NHEJ resulting in persistence of DNA damages.

Interaction between BRCA1 and ER-α might regulate DNA-DSB repair

Our results demonstrate that haploinsufficiency of either BRCA1 or ER-α and associated interruption in E2-ER signaling might alter the DDR events in breast cancer cells. Thus we analyzed the possibility of protein-protein interaction between ER-α and BRCA1 during DNA damage repair. A strong interaction between ER-α and BRCA1 proteins were observed in MCF-7 cells during DNA-DSB repair, which gradually declined by about 48 hours as analyzed by *in situ* PLA (**Figure 7I**).

Interaction between ER-α and BRCA1 was significantly higher in ER-α^+ human breast tumor tissues as well, when compared to adjacent normal tissues (**Figure 7J**) which might be suggestive of the persisting damages in tumor cells and the allied interaction between ER-α and BRCA1 during damage repair. The results were also substantiated with co-immunoprecipitation of BRCA1 and ER-α using lysate from DSB induced MCF-7 cells (**Figure 7K**). These results signify that BRCA1 and ER-α proteins interact with each other during DNA-DSB repair in ER-α^+ breast cancer cells.

We also observed apparent differences in nuclear to cytoplasmic ratio of functional ER-α protein as analyzed by western blot analysis in MCF-7 cells post cisplatin induced DSB and follow on recovery period from 0-48 hours. As an immediate response to DSB, in comparison to cytoplasmic expression, a significant increase in the nuclear expression of ER-α protein (0-24 hours) was observed. However, with an increase in rescue period, an inversion in ratio was observed with increased expression of ER-α in cytoplasmic fraction compared to the nuclear fraction (**Figure 7L**, **7M**). We could also observe nuclear co-localization of ER-α and BRCA1 proteins during DNA-DSB repair (**Figure 7N**).

Thus, we demonstrate that the cytoplasmic to nuclear localization of ER-α and its consequent co-localization and interaction with BRCA1 protein is important in DNA-DSB repair.

ER-α deficiency modulate BRCA1 regulated oxidative damage repair

In addition to HRR, BRCA1 is reported to be a major regulator of the oxidative damage coupled BER pathway as well. Furthermore, our GeneMANIA analysis had shown that several BER proteins interact with both BRCA1 and ER-α (Table S1). Therefore, we analyzed whether ER-α activity can also regulate BER in breast cancer cells. For this, we exogenously induced repairable oxidative damage in ER-α^+ and ER-α^- cells using 300 μM H_2O_2/30 mins and scored the expression, localization and kinetics of OGG1, (Oxo-guanidine glycosylase) a major regulator and indicator of efficient BER pathway. 300 μM H_2O_2 did not result in significant cell death, but induced 8-OXO-G base lesion in the cells (Figure S5D, S5E). The ER-α as well as BRCA1 deficient cells did not show any significant difference in OGG1 mRNA expression upon H_2O_2 treatment and retained the OGG1 protein only to cytoplasm. siRNA mediated silencing of either ER-α/BRCA1 or both in MCF-7 cells, further reduced the nuclear recruitment and expression of OGG1 protein (**Figure 8A**). OGG1 expression increased upon H_2O_2 treatment in MCF-7 cells and these cells exhibited a timely nuclear recruitment and gradual decline of OGG1 upon post treatment rescue. Concomitant results were observed with MDA-MB-231 cells as well (**Figure 8B-D**). Presence of OGG1 in cells on exposure to oxidative damage is a hallmark of efficient base excision repair (BER) and its altered expression is reported in many cancers [33].

The OGG1 expression in response to H_2O_2 induced damage did not show any significant difference between MDA-MB-231 cells (ER-α^- BRCA1 wild type) and MDA-MB-231shBRCA1 (ER-α^- BRCA1 deficient) cells as analyzed by qRTPCR (See **Figure 8D**). Concomitantly, we could also observe a higher expression of 8-OXO-G lesion and considerably lower expression of OGG1 in ER-α^- breast tumor tissues in comparison with ER-α^+ tissues, as analyzed by IHC (**Figure 8E**). Thus, these results indicate that functional ER-α might also augment BRCA1 mediated oxidative damage repair in estrogen responsive cells.

As BRCA1 knock down did not influence OGG1 expression in MDA-MB-231shBRCA1 cells compared to the control cells, we further analyzed the BRCA1 expression in response to oxidative damage. An induction in expression of BRCA1 was observed upon damage in MCF-7 cells, but not in ER-α deficient MDA-MB-231

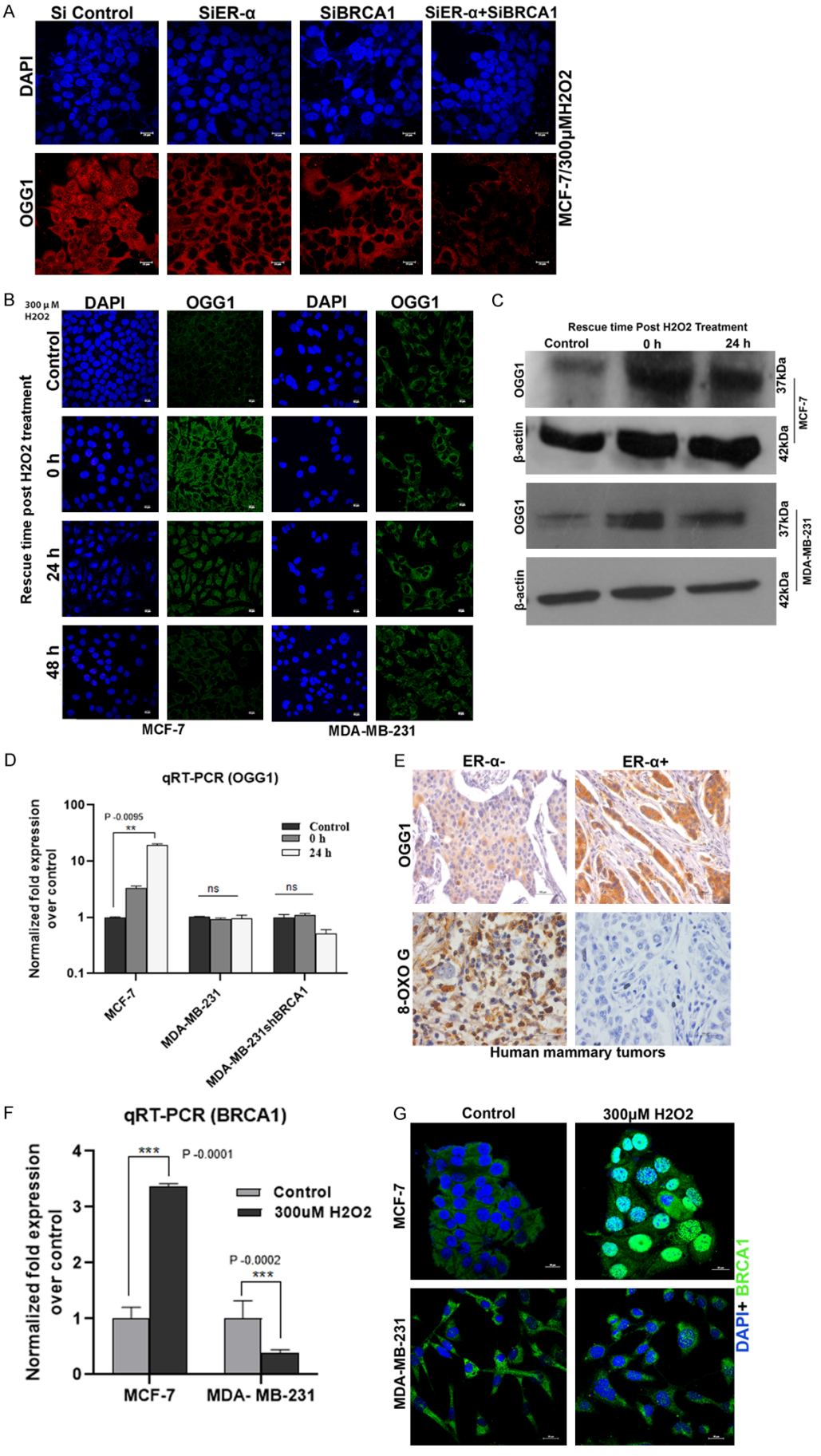
A
Si Control
SiER-α
SiBRCA1
SiER-α+SiBRCA1
DAPI
OGG1
MCF-7/300μMH2O2
B
300 μ M H2O2
DAPI
OGG1
DAPI
OGG1
Rescue time post H2O2 treatment
Control
0 h
24 h
48 h
MCF-7
MDA-MB-231
C
Rescue time Post H2O2 Treatment
Control
0 h
24 h
OGG1
37kDa
β-actin
42kDa
MCF-7
OGG1
37kDa
β-actin
42kDa
MDA-MB-231
D
qRT-PCR (OGG1)
Normalized fold expression over control
P -0.0095
**
ns
ns
Control
0 h
24 h
MCF-7
MDA-MB-231
MDA-MB-231shBRCA1
E
ER-α-
ER-α+
OGG1
8-OXO G
Human mammary tumors
F
qRT-PCR (BRCA1)
Normalized fold expression over control
***
P -0.0001
P -0.0002
***
Control
300uM H2O2
MCF-7
MDA- MB-231
G
Control
300μM H2O2
MCF-7
MDA-MB-231
DAPI+ BRCA1

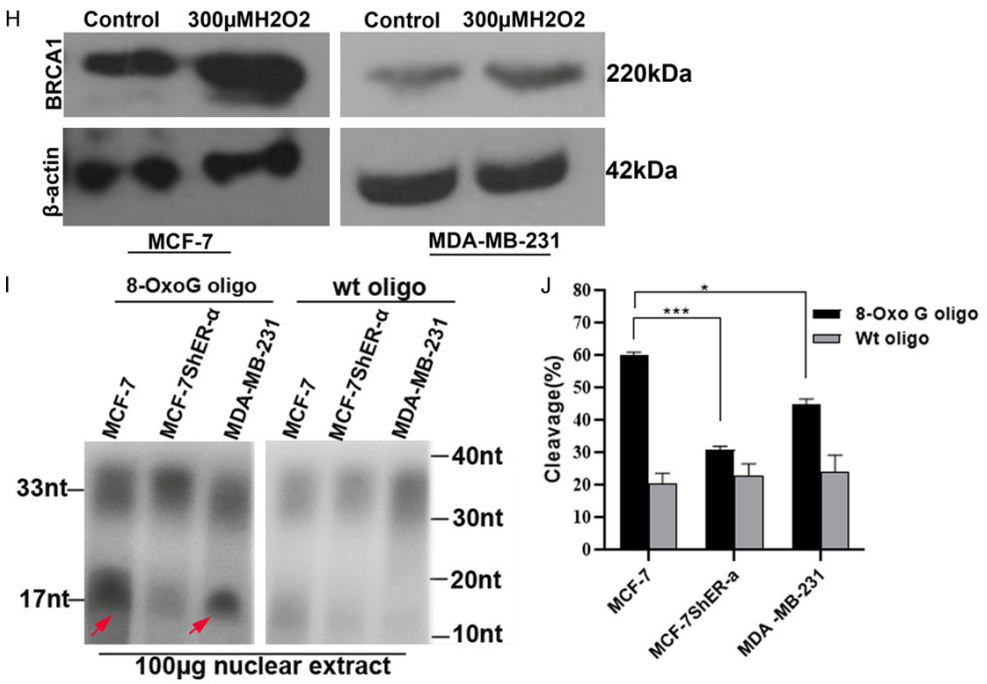

Figure 8. ER-α deficiency alters BRCA1 regulated oxidative damage repair: (A) Immmunofluorescence staining of OGG1 in MCF-7SiER-α and MCF-7SiBRCA1 cells upon 300 μM H_2O_2 induced oxidative damage (60X, Scale bar-20 μm). (B) Immmunofluorescence staining of OGG1 in response to 300 μM H_2O_2 induced oxidative damage in MCF-7 and MDA-MB-231 cells, scored at different time points of rescue. (C) Western blot analysis and (D) qRTPCR of OGG1 in MCF-7, MDA-MB-231 and MDA-MB-231shBRCA1 cells upon 300 μM H_2O_2 treatment. (E) IHC staining of OGG1 and 8-OXO-G in ER-α$^-$ and ER-α$^+$ human breast tumor tissues (20X, scale bar 100 μm, ER-α$^-$/ER-α$^+$ tissue, n=4). (F) qRTPCR analysis, (G) Immmunofluorescence staining and (H) western blot analysis of BRCA1, respectively in MCF-7 and MDA-MB-231 upon H_2O_2 induced oxidative damage. (I, J) Oligonucleotide Inscision Assay: Actively growing MCF-7, MCF-7shER-α and MDA-MB-231 cells were treated with 300 μM H_2O_2 to induce oxidative damage, 100 μg nuclear extracts from the damage induced cells, were tested for their ability to incise duplex oligonucleotides (oligo) containing a 8-OXO-G lesion. Corresponding wild-type duplex oligonucleotide was used as control (I) shows the representative DNA gel and (J) is the quantitative extents of cleavage.

cells (**Figure 8F-H**). We also observed reduced BER efficiency and cleavage activity (potent marker of BER activity) in ER-α deficient cells as analyzed by BER assay using modified-labeled oligonucleotides (**Figure 8I**, **8J**). This implies that the regulation of oxidative damage response by BRCA1 is largely dependent on E2-ER signaling.

ER-α deficient cells failed to eliminate damage induced senescent cells

Persistent unrepaired DSBs can trigger DDR and lead to cellular senescence which is a state of irreversible metabolic dormancy. Hence, we further checked whether the long term persistence of DNA lesions observed with ER-α deficient cells lead to cellular senescence. For this we analyzed the SA-β-gal activity of these cells post cisplatin treatment. Upon DNA-DSB induction, MDA-MB-231 cells elicited significantly higher SA-β-gal activity (**Figure 9A**), with gradual increase in percentage of positively stained cells on post treatment rescue. The expression of senescent markers P^{15} and P^{16} were also found to be higher in these cells in comparison with MCF-7 cells (**Figure 9B**, **9C**). This indicates that ER-α deficiency leads to impaired or delayed damage repair and directs a higher percentage of cells to undergo a state of cellular senescence.

Further to evaluate whether these population of senescent cells will be eliminated from cell cycle, we incubated the cisplatin treated DSB induced MDA-MB-231 and MCF-7 cells in complete growth media post treatment and allowed to grow for 15 days in 3 passages. Even with a longer recovery period, MDA-MB-231 cells showed considerably higher percentage of per-

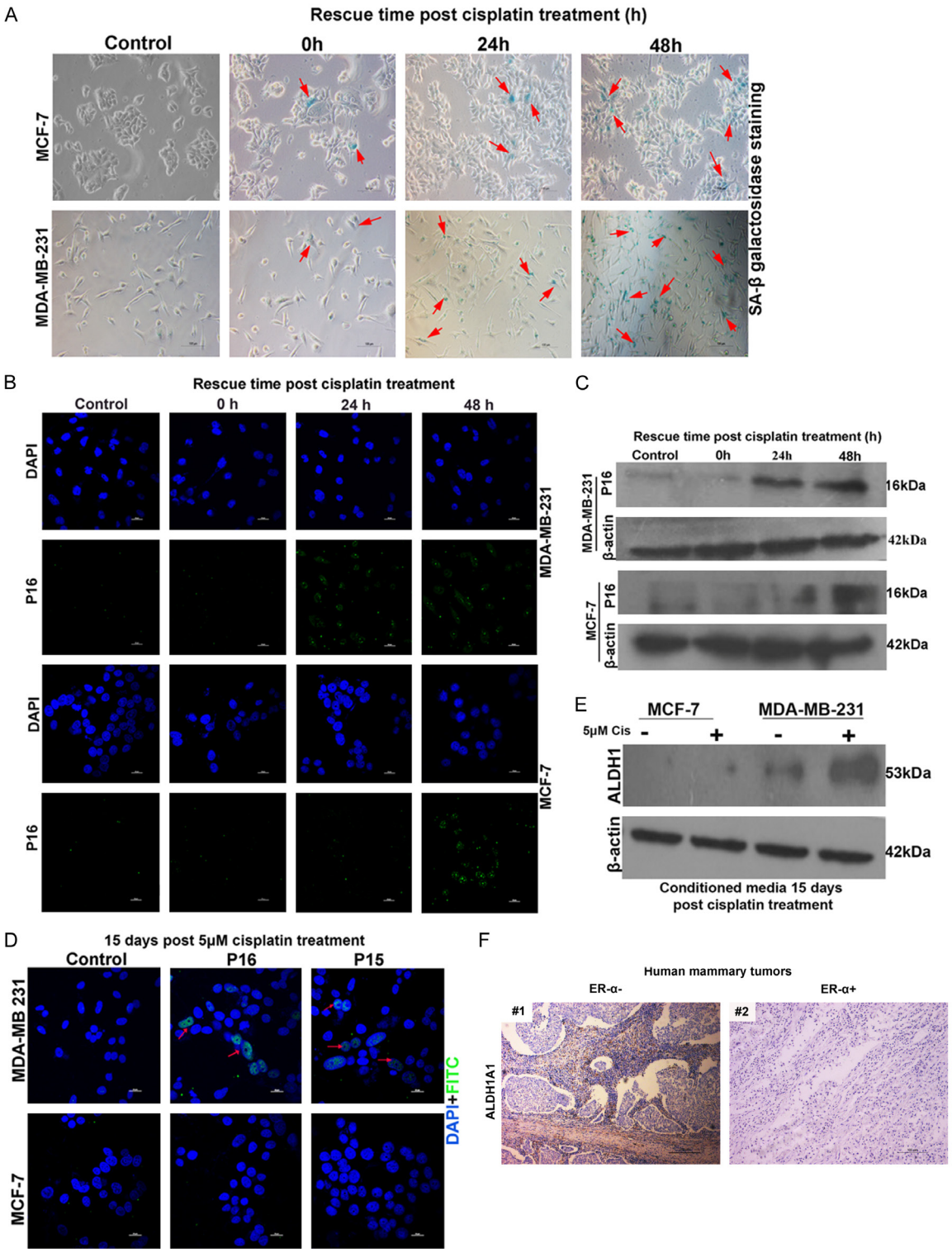

Figure 9. ER-α deficient cells failed to eliminate damage induced senescent cells. (A) SA-β-gal staining of MCF-7 and MDA-MB-231 analyzed at different time posts of post treatment rescue. Cells stained blue-green indicated with red arrows are positively stained (20X, Scale bar 100 μm). (B) Immmunofluorescence staining and (C) Western blot analysis for the senescence biomarker p16, respectively in MDA-MB-231cells and MCF-7 cells, upon cisplatin induced DNA-DSB and post treatment rescue. (D) MDAMB-231 and MCF-7 cells showing, presence of P16 and P15 expressing cells after 15 days of rescue and 3 passages post cisplatin induced DSB, as analyzed by immunocytochemistry. (E) Western blot analysis showing expression of ALDH1 in the condition media of MCF-7 and MDA-MB-231 cells, 15 days post cisplatin treatment. (F) IHC analysis of ALDH1 in ER-α$^-$ and ER-α$^+$ human breast tumor tissues (10X, Scale bar 100 μm).

sisting P^{15} and P^{16} positive cells in comparison with MCF-7cells (**Figure 9D**). This indicates that ER-α^- cells elicited delayed/impaired elimination of senescent cells from the system.

It is reported that the long term persistence of damage induced senescent cells have a distinct secretome which would modify their environment, and allow them to undergo transformation or de-differentiation to an aggressive CSC like phenotype and the persistence of such cells could finally lead to disease recurrence [34, 35].

In support of this, we could also observe a higher expression of the CSC marker ALDH1 in the conditioned media (Secretome) of MDA-MB-231 cells as analyzed by western blot analysis 15 days post cisplatin treatment (**Figure 9E**). Moreover, ER-α^- human breast tumor tissues also showed significantly higher ALDH1 expression in comparison with ER-α^+ tissues as analyzed by IHC (**Figure 9F**). This evidence suggests the persistence of a smaller population of reprogrammed-senescent cells or CSC residing within the ER-α^- tumors (possibly explaining the aggressiveness and recurrence associated with ER-α^- tumors).

Thus taken together, we have demonstrated that ER-α plays pivotal role in the DDR signaling cascades, triggering the BRCA1 mediated high fidelity DNA damage repair in breast cancer cells. Furthermore, deregulation of ligand dependent ER-α transactivation impeded high-fidelity repair pathways like HRR and BER and promoted the repair through error prone pathway like NHEJ. This could lead to the persistence of DNA damage and transformation of cells to an aggressive phenotype conducive to tumorigenesis. Therefore, we report that functional ER-α and regulated ER-α signaling augment BRCA1 mediated DNA damage repair.

Discussion

BRCA1 related tumors are mostly TNBCs exhibiting a high degree of chromosomal defects and are generally restricted to estrogen responsive tissues. We evaluated the role of ER-α in BRCA1 regulated DDR pathways and how it could influence the process of tumorigenesis as BRCA1 is an E2-ER responsive gene and recent studies mark the influence of ER-α signaling in eukaryotic DDR.

Directly scoring the damage repair events inherent to the cell might be tricky, as the parameters scored at the innate level may not hit measureable/detectable threshold and might not provide quantitative description. Thus, the present study utilized a platform of exogenously inducing repairable DSBs in cell lines using the DNA damaging agent cisplatin. Induction of DNA-DSB using specific concentration of cisplatin triggered the DDR in cells with activation of DSB repair proteins including BRCA1. Most surprisingly, concurrent increase and gradual decline in the expression of functional ER-α was observed in response to DSB. GeneMANIA analysis endorsed role of ER-α, where we could see several DDR regulators independently interacting with both BRCA1 and ER-α giving initial evidence on the possible role of ER-α activity in DDR.

Activated DDR is a cascade with sequential recruitment of sensors, transducers and effectors orchestrating an appropriate repair of DNA damage and thus resolving DNA replication problems. Our finding that the ER-α is a major facilitator of BRCA1 mediated repairs came from the scoring of γH2AX kinetics which is one of the early events and the hallmarks of DSB repair [36-38] in breast cancer cells post DSB induction. Wild type cells with functional ER-α repaired the exogenously induced DNA-DSB with gradual decline in the γH2AX expression. On the contrary, knockdown or deficiency of ER-α resulted in persistent activation of γH2AX, which is an indication of impeded DSB repair. However, reintroduction of wild-type ER-α in ER deficient cells effectively rescued the cells from exogenously induced DNA-DSB.

Knockdown of wild type BRCA1, or introduction of wild type BRCA1 to BRCA1 mutant cells did not influence the kinetics and long term persistence of damage induced γH2AX foci in ER-α deficient cells. The biochemical interaction between γH2AX and BRCA1 at damage site and the consequential removal of γH2AX by BRCA1 after damage repair are critical events in DDR [39]. Moreover, the retention of DSB induced γ-H2AX foci for more than 24 hours is considered as an indication of delayed or impaired DSB repair [37, 38]. Thus, we demonstrate that functional ER-α has regulatory role in augmenting the BRCA1 mediated cellular response to DNA-DSB.

There was no significant difference in the delayed DDR elicited by ER-α deficient cells, even with the introduction of wild-type p53. A possible explanation for this might be that; active ER-α signaling is known to suppress p53 activity in estrogen responsive cells, on the contrary, BRCA1 can regulate mitogenic activities due to active ER-α activity [25, 26, 40, 41]; Thus, in cases of BRCA1 haploinsufficiency or mutation, BRCA1 might reverse the control over ER-α signaling, thereby stimulating NHEJ and suppressing HRR. In such cases, ER-α which is not under the BRCA1 surveillance, down regulates p53 activity and directs uncontrolled cell proliferation in Cyclin D1 dependent manner. In estrogen non-responsive BRCA1 wild type cells, inhibition of p53 by ER-α might not exist; therefore, p53 might be the major mediator of DDR, instead of ER-α. Where, deficiency of ER-α up-regulates Ku80, which stimulates uncontrolled NHEJ in these cells. However, the up-regulation of error prone NHEJ might not affect the cell survival, if these estrogen non-responsive cells are wild type for BRCA1 as well as p53; while, the loss of both BRCA1 and p53, questions the genomic stability. Together indicating that, ER-α signaling can augment BRCA1 functions in estrogen responsive cells, thus, the loss of BRCA1 along with deregulation of ER-α signaling together affect the chromosomal integrity.

Conditional deregulation of ER-α signaling *in vitro*, by depriving ligand E2 or receptor ER-α revealed the fundamental role of ER-α activity in DDR. While E2 deprivation increased ER-α expression, the tamoxifen treatment decreased ER-α activity, but both these conditions delayed DDR; indicating that over-expression of functional ER-α might not augment DDR whereas a functional E2-ER signaling can. Thus, for the first time we report that ligand-dependent ER-α signaling modulate BRCA1 regulated DDR in breast cancer cells, whereas ligand-independent transactivation allows the cells to adapt and re-grow in E2 deprivation [42]. There are reports stating that the ligand-independent transactivation of ER-α cannot retain all the ER-α functions but fuel tumorigenesis in the proliferating cells [27], which is in agreement with our hypothesis that uncontrolled ER-α signaling can deregulate DDR and trigger tumorigenesis. Thus, it is evident that the pro-proliferative and anti-apoptotic arms of DDR might be regulated by ligand-dependent ER-α signaling.

Expression and localization of decisive molecules of DSB repair pathways (NHEJ/HRR); pS988-BRCA1, 53BP1 and other DDR effectors like MRN complex proteins were impeded in ER-α deficiency, signifying that the choice of DSB repair pathway is also influenced by ER-α status. BRCA1-S^{988} phosphorylation is specific to trigger DSB repair, particularly through HRR pathway [43], whereas, 53BP1 promote repair through NHEJ [28]. Absence of BRCA1 phosphorylations at S^{1524} and S^{1423} and precise kinetics of p S988-BRCA1 observed with ER-α proficient cells in response to DSB signifies an active HRR and intact DSB repair. Higher expression of HRR regulators like pS988-BRCA1 and RAD50, but not 53BP1 in ER-α^+ treatment naive human breast cancer tissues in comparison with ER-α^- tissues further validate the perception that a condition of ER-α deficiency or deregulated E2-ER signaling might compromise the HRR in cells thereby activating 53BP1 like effectors and facilitating the repair through error prone pathways like a-NHEJ (alternative NHEJ-error prone pathway). Higher and persistent expression of 53BP1 visualized with damage induced MCF-7 cells should not be misinterpreted , as we have used asynchronously proliferating cells for the assay and NHEJ is reported to be active throughout the cell cycle [29].

It was also apparent that deregulated ER-α signaling not only compromised the HRR but also reduced the damage recovery and associated colonigenic potential of cells *in vitro*. Conversely, ER-α deficiency facilitated the DSB repair through an activated NHEJ pathway with stimulated expression of regulators like KU80 and DNA-PK.

While ER-α or BRCA1 deficiency limited the DSB repair, our protein interaction studies demonstrated direct interaction between ER-α and BRCA1 proteins facilitating the DSB repair. Increased cytoplasmic to nuclear expression of ER-α protein in response to DSB and higher percentage protein interaction observed in breast tumor tissues evidently suggest the role of ER-α activity in high-fidelity DNA-DSB repair pathways.

The BRCA1 regulated BER pathway was also found to be significantly affected in conditions of ER-α deficiency with higher persistence of 8-OXO-G lesion and lower expression and delayed nuclear localization of OGG1 enzyme.

These cells also elicited reduced cleavage activity signifying a compromised BER. Depleted expression and mutation of OGG1 is reported to activate the multistage process of carcinogenesis in lung/kidney/mammary cells [44]. A study published in 2020 in nucleic acid research also demonstrates that OGG1 expression is of considerable importance and can be considered to be a potent target for cancer treatments [45]. OGG1 not only repair or remove lesions but also promote cell death, eliminate malignant cells and maintains genomic stability [46]; and thus, aberrant expression of OGG1 is always correlated to malignancies.

Deficiency in ER-α/BRCA1 or both consistently delayed cell cycle progression. ER-α deficient cells were lagging behind the ER-α proficient cells in sensing and repairing the damage and as a result elicited an altered cell cycle with prolonged G2/M arrest. These cells also exhibited higher degree of chromosomal defects.

Our results were thus consistent with the speculation that persisting lesions, delayed damage repair, defective high-fidelity pathways and altered cell cycle events create a niche for the generation of tumor initiating cells triggering tumorigenesis years later. This apparently indicates that while BRCA1 is the sentinel for DNA-DSB repair, functional ER-α and a regulated ligand dependent ER-α signaling might be indispensible for a controlled DDR in breast cancer cells. This can be correlated to the late onset of breast cancers in post menopausal women as age related hormonal imbalance or BRCA1 mutations gradually trigger the aforesaid precancerous events and fuel tumorigenesis.

The reduced efficiency of ER-α deficient cells to repair DNA-DSB and eliminate the damaged cells, generated a sub-population of persisting senescent cells. It is reported that long term persistence of senescent cells in the system gradually leads to their de-diferenciation, reprogramming them to an aggressive stem-cell like phenotype and facilitating their re-entry into cell cycle thus initiating tumorigenesis in future [35, 47]. The presence of CSC or differentiation marker ALDH1A1 observed in the secretome of these senescent cells, further substantiate this notion. Moreover, significantly higher ALDH1 expression was detected in ER-α^- tissues in comparison with ERα^+ human breast tumor tissues. This is suggestive of the persistence of a concealed population of reprogrammed-senescent cells or CSCs residing within the ER-α^- tumors; which, can be correlated to the higher percentage of disease recurrence and aggressiveness associated with TNBCs. Thus, it can be speculated that the reduced ER-α expression observed in tissues of post menopausal women and BRCA1 mutation carriers might be correlated to their enhanced risk towards breast and ovarian cancers.

DDR is considered to be a barrier against genomic instability and malignant transformation. Our work shows that cell differentiation and reprogramming is achieved through defective DDR machinery and the importance of DNA-DSB repair in tumorigenesis has to be reconsidered.

We could also observe disparity in gene expression of different repair genes between ER-α deficient and proficient cells upon analyzing a panel of 84 mammalian DDR genes, which was further substantiated with the data from the METABRIC data set TCGA, Oncomine (Unpublished Data, data not shown).

Any endogenous or exogenous factors affecting ER-α signaling might thus sensitize the cells towards genomic insults. Thus, the contemporary clinical practices of endocrine or hormone deprivation therapy which inhibits ER-α activity, with the use of SERMs could be reconsidered as it might result in persistent activation of DNA-DSBs. Higher cancer recurrences and increased incidence of endometrial cancers associated with long term tamoxifen usage is a prime illustration of this fact [48, 49].

Thus, the association between central components of DDR and ER-α signaling is a definite possibility and further studies on this regard can open up new avenues for the prevention and therapies of estrogen-sensitive proliferative diseases particularly in management of BRCA1 associated cancers. Analyzing a large panel of DDR associated biomarkers with regard to ER signaling is a necessity as this enables us to identify many druggable targets for the management of HBOCs.

Conclusion

Deregulated Estrogen signaling resulting from ER-α/BRCA1 deficiency, age/hormone related or clinicopathological condition can induce DNA damage via the production of oxidative metabolites [7]. We report that interrupted estrogen signaling also aggravates excessive proliferation in cells leading to insufficient time for repair, deregulated DDR pathways and defective cell cycle progression. Deregulated ER-α signaling compromised the BRCA1 mediated high fidelity pathways like HRR and BER and facilitated repair via error prone pathways like NHEJ. This lead to retention of DNA damages in cells, transforming them to an aggressive phenotype and triggering a pre-cancerous environment. Thus, we report that ER-α activity is indispensible for BRCA1 mediated DDR and maintenance of genomic integrity.

Acknowledgements

P.S. acknowledges the financial support from Indian Council for Medical Research, Government of India (53/20/2012-BMS) and Science and Engineering Research Board, Department of Science and Technology, Government of India (EMR/2017/002222), as well as the intra mural funding from Rajiv Gandhi Centre for Biotechnology, Thiruvananthapuram, Kerala, India. The authors acknowledge Department of Science and Technology (DST-INSPIRE), Government of India for the Senior Research Fellowship to A.R., Rajiv Gandhi Centre for Biotechnology, Thiruvananthapuram, Kerala, India for Research fellowship to R.N & A.V.W, Indian Council for Medical Research, Government of India for the Senior Research Fellowship to N.R.L, Council of Scientific and Industrial Research, India for research fellowship to GRV. The University Grants Commission, Government of India for Senior Research Fellowship to N.K & D.P, The authors also acknowledge University of Kerala, Thiruvananthapuram for supporting the research work. The authors acknowledge Dr. Radhika Nair, Scientist, Rajiv Gandhi Centre for Biotechnology, for her critical comments and proof reading the manuscript. This research was funded by Indian Council for Medical Research Govt. of India. (ICMR.No:53/20/2012-BMS).

Disclosure of conflict of interest

None.

Address correspondence to: Dr. Priya Srinivas, Scientist-F, Cancer Research Program, Rajiv Gandhi Centre for Biotechnology, Thiruvananthapuram 695014, Kerala, India. Tel: +91-4712529495; E-mail: priyasrinivas@rgcb.res.in

References

[1] Ratanaphan A. A DNA repair BRCA1 estrogen receptor and targeted therapy in breast cancer. Int J Mol Sci 2012; 13: 14898-14916.

[2] Wang L and Di LJ. BRCA1 and estrogen/estrogen receptor in breast cancer: where they interact? Int J Biol Sci 2014; 10: 566-575.

[3] Fan S, Ma YX, Wang C, Yuan RQ, Meng Q, Wang JA, Erdos M, Goldberg ID, Webb P, Kushner PJ, Pestell RG and Rosen EM. Role of direct interaction in BRCA1 inhibition of estrogen receptor activity. Oncogene 2001; 20: 77-87.

[4] Ma Y, Fan S, Hu C, Meng Q, Fuqua SA, Pestell RG, Tomita YA and Rosen EM. BRCA1 regulates acetylation and ubiquitination of estrogen receptor-alpha. Mol Endocrinol 2010; 24: 76-90.

[5] Jeffy BD, Hockings JK, Kemp MQ, Morgan SS, Hager JA, Beliakoff J, Whitesell LJ, Bowden GT and Romagnolo DF. An estrogen receptor-alpha/p300 complex activates the BRCA-1 promoter at an AP-1 site that binds Jun/Fos transcription factors: repressive effects of p53 on BRCA-1 transcription. Neoplasia 2005; 7: 873-882.

[6] Wei L, Lan L, Yasui A, Tanaka K, Saijo M, Matsuzawa A, Kashiwagi R, Maseki E, Hu Y, Parvin JD, Ishioka C and Chiba N. BRCA1 contributes to transcription-coupled repair of DNA damage through polyubiquitination and degradation of Cockayne syndrome B protein. Cancer Sci 2011; 102: 1840-1847.

[7] Caldon CE. Estrogen signaling and the DNA damage response in hormone dependent breast cancers. Front Oncol 2014; 4: 106.

[8] Matta J, Morales L, Ortiz C, Adams D, Vargas W, Casbas P, Dutil J, Echenique M and Suarez E. Estrogen receptor expression is associated with DNA repair capacity in breast cancer. PLoS One 2016; 11: e0152422.

[9] Snouwaert JN, Gowen LC, Latour AM, Mohn AR, Xiao A, DiBiase L and Koller BH. BRCA1 deficient embryonic stem cells display a decreased homologous recombination frequency and an increased frequency of non-homologous recombination that is corrected by expression of a brca1 transgene. Oncogene 1999; 18: 7900-7907.

[10] Ma Y, Hu C, Riegel AT, Fan S and Rosen EM. Growth factor signaling pathways modulate BRCA1 repression of estrogen receptor-alpha activity. Mol Endocrinol 2007; 21: 1905-1923.

[11] Modrich P and Lahue R. Mismatch repair in replication fidelity, genetic recombination, and

cancer biology. Annu Rev Biochem 1996; 65: 101-133.
[12] Hemalatha SK, Sengodan SK, Nadhan R, Dev J, Sushama RR, Somasundaram V, Thankappan R, Rajan A, Latha NR, Varghese GR, Mathew AP, Somanathan T and Srinivas P. Brcal defective breast cancer cells induce in vitro transformation of cancer associated fibroblasts (CAFs) to metastasis associated fibroblasts (MAF). Sci Rep 2018; 8: 13903.
[13] Howe B, Umrigar A and Tsien F. Chromosome preparation from cultured cells. J Vis Exp 2014; e50203.
[14] Nikolova T, Ensminger M, Lobrich M and Kaina B. Homologous recombination protects mammalian cells from replication-associated DNA double-strand breaks arising in response to methyl methanesulfonate. DNA Repair (Amst) 2010; 9: 1050-1063.
[15] Pierce AJ, Johnson RD, Thompson LH and Jasin M. XRCC3 promotes homology-directed repair of DNA damage in mammalian cells. Genes Dev 1999; 13: 2633-2638.
[16] Wu J, Zhang X, Zhang L, Wu CY, Rezaeian AH, Chan CH, Li JM, Wang J, Gao Y, Han F, Jeong YS, Yuan X, Khanna KK, Jin J, Zeng YX and Lin HK. Skp2 E3 ligase integrates ATM activation and homologous recombination repair by ubiquitinating NBS1. Mol Cell 2012; 46: 351-361.
[17] Iliakis G, Rosidi B, Wang M and Wang H. Plasmid-based assays for DNA end-joining in vitro. Methods Mol Biol 2006; 314: 123-131.
[18] Zhong Q, Boyer TG, Chen PL and Lee WH. Deficient nonhomologous end-joining activity in cell-free extracts from Brca1-null fibroblasts. Cancer Res 2002; 62: 3966-3970.
[19] Saha T, Smulson M and Rosen EM. BRCA1 regulation of base excision repair pathway. Cell Cycle 2010; 9: 2471-2472.
[20] Nyaga SG, Lohani A, Jaruga P, Trzeciak AR, Dizdaroglu M and Evans MK. Reduced repair of 8-hydroxyguanine in the human breast cancer cell line, HCC1937. BMC Cancer 2006; 6: 297.
[21] Montojo J, Zuberi K, Rodriguez H, Kazi F, Wright G, Donaldson SL, Morris Q and Bader GD. GeneMANIA Cytoscape plugin: fast gene function predictions on the desktop. Bioinformatics 2010; 26: 2927-2928.
[22] Wu J, Lu LY and Yu X. The role of BRCA1 in DNA damage response. Protein Cell 2010; 1: 117-123.
[23] Jang ER and Lee JS. DNA damage response mediated through BRCA1. Cancer Res Treat 2004; 36: 214-221.
[24] Hybiak J, Domagala P and Domagala W. BRCA1 and PARP1 mRNA expression during progression from normal breast to ductal carcinoma in situ and invasive breast cancer: a laser microdissection study. Pol J Pathol 2018; 69: 347-355.
[25] Swetzig WM, Wang J and Das GM. Estrogen receptor alpha (ERalpha/ESR1) mediates the p53-independent overexpression of MDM4/MDMX and MDM2 in human breast cancer. Oncotarget 2016; 7: 16049-16069.
[26] Berger C, Qian Y and Chen X. The p53-estrogen receptor loop in cancer. Curr Mol Med 2013; 13: 1229-1240.
[27] Jeng MH, Shupnik MA, Bender TP, Westin EH, Bandyopadhyay D, Kumar R, Masamura S and Santen RJ. Estrogen receptor expression and function in long-term estrogen-deprived human breast cancer cells. Endocrinology 1998; 139: 4164-4174.
[28] Gupta A, Hunt CR, Chakraborty S, Pandita RK, Yordy J, Ramnarain DB, Horikoshi N and Pandita TK. Role of 53BP1 in the regulation of DNA double-strand break repair pathway choice. Radiat Res 2014; 181: 1-8.
[29] Mao Z, Bozzella M, Seluanov A and Gorbunova V. DNA repair by nonhomologous end joining and homologous recombination during cell cycle in human cells. Cell Cycle 2008; 7: 2902-2906.
[30] Parameswaran B, Chiang HC, Lu Y, Coates J, Deng CX, Baer R, Lin HK, Li R, Paull TT and Hu Y. Damage-induced BRCA1 phosphorylation by Chk2 contributes to the timing of end resection. Cell Cycle 2015; 14: 437-448.
[31] Cuozzo C, Porcellini A, Angrisano T, Morano A, Lee B, Di Pardo A, Messina S, Iuliano R, Fusco A, Santillo MR, Muller MT, Chiariotti L, Gottesman ME and Avvedimento EV. DNA damage, homology-directed repair, and DNA methylation. PLoS Genet 2007; 3: e110.
[32] Richardson C, Moynahan ME and Jasin M. Double-strand break repair by interchromosomal recombination: suppression of chromosomal translocations. Genes Dev 1998; 12: 3831-3842.
[33] Kumagae Y, Hirahashi M, Takizawa K, Yamamoto H, Gushima M, Esaki M, Matsumoto T, Nakamura M, Kitazono T and Oda Y. Overexpression of MTH1 and OGG1 proteins in ulcerative colitis-associated carcinogenesis. Oncol Lett 2018; 16: 1765-1776.
[34] Ouchi R, Okabe S, Migita T, Nakano I and Seimiya H. Senescence from glioma stem cell differentiation promotes tumor growth. Biochem Biophys Res Commun 2016; 470: 275-281.
[35] Sharpless NE. The persistence of senescence. Sci Aging Knowledge Environ 2003; 2003: PE24.
[36] Ivashkevich A, Redon CE, Nakamura AJ, Martin RF and Martin OA. Use of the gamma-H2AX assay to monitor DNA damage and repair in translational cancer research. Cancer Lett 2012; 327: 123-133.

[37] Varvara PV, Karaolanis G, Valavanis C, Stanc G, Tzaida O, Trihia H, Patapis P, Dimitroulis D and Perrea D. gamma-H2AX: a potential biomarker in breast cancer. Tumour Biol 2019; 41: 1010428319878536.
[38] Kinner A, Wu W, Staudt C and Iliakis G. Gamma-H2AX in recognition and signaling of DNA double-strand breaks in the context of chromatin. Nucleic Acids Res 2008; 36: 5678-5694.
[39] Krum SA, la Rosa Dalugdugan E, Miranda-Carboni GA and Lane TF. BRCA1 forms a functional complex with gamma-H2AX as a late response to genotoxic stress. J Nucleic Acids 2010; 2010: 801594.
[40] Lion M, Bisio A, Tebaldi T, De Sanctis V, Menendez D, Resnick MA, Ciribilli Y and Inga A. Interaction between p53 and estradiol pathways in transcriptional responses to chemotherapeutics. Cell Cycle 2013; 12: 1211-1224.
[41] Reich NC and Levine AJ. Growth regulation of a cellular tumour antigen, p53, in nontransformed cells. Nature 1984; 308: 199-201.
[42] Santen RJ, Song RX, Zhang Z, Kumar R, Jeng MH, Masamura A, Lawrence J Jr, Berstein L and Yue W. Long-term estradiol deprivation in breast cancer cells up-regulates growth factor signaling and enhances estrogen sensitivity. Endocr Relat Cancer 2005; 12 Suppl 1: S61-73.
[43] Zhang J, Willers H, Feng Z, Ghosh JC, Kim S, Weaver DT, Chung JH, Powell SN and Xia F. Chk2 phosphorylation of BRCA1 regulates DNA double-strand break repair. Mol Cell Biol 2004; 24: 708-718.
[44] Ali K, Mahjabeen I, Sabir M, Mehmood H and Kayani MA. OGG1 mutations and risk of female breast cancer: meta-analysis and experimental data. Dis Markers 2015; 2015: 690878.
[45] Visnes T, Benitez-Buelga C, Cazares-Korner A, Sanjiv K, Hanna BMF, Mortusewicz O, Rajagopal V, Albers JJ, Hagey DW, Bekkhus T, Eshtad S, Baquero JM, Masuyer G, Wallner O, Muller S, Pham T, Gokturk C, Rasti A, Suman S, Torres-Ruiz R, Sarno A, Wiita E, Homan EJ, Karsten S, Marimuthu K, Michel M, Koolmeister T, Scobie M, Loseva O, Almlof I, Unterlass JE, Pettke A, Bostrom J, Pandey M, Gad H, Herr P, Jemth AS, El Andaloussi S, Kalderen C, Rodriguez-Perales S, Benitez J, Krokan HE, Altun M, Stenmark P, Berglund UW and Helleday T. Targeting OGG1 arrests cancer cell proliferation by inducing replication stress. Nucleic Acids Res 2020; 48: 12234-12251.
[46] Wang R, Li C, Qiao P, Xue Y, Zheng X, Chen H, Zeng X, Liu W, Boldogh I and Ba X. OGG1-initiated base excision repair exacerbates oxidative stress-induced parthanatos. Cell Death Dis 2018; 9: 628.
[47] Overholtzer M. Senescent cells feed on their neighbours. Nature 2019; 574: 635-636.
[48] Lee M, Piao J and Jeon MJ. Risk factors associated with endometrial pathology in premenopausal breast cancer patients treated with Tamoxifen. Yonsei Med J 2020; 61: 317-322.
[49] Emons G, Mustea A and Tempfer C. Tamoxifen and endometrial cancer: a Janus-headed drug. Cancers (Basel) 2020; 12: 2535.

Table S1. GeneMANIA online tool

BER	NER	MMR	HR	NHEJ
NEIL3, UNG, TDG, POLL, HMGB1 & PARP1	CUL4B, DDB2,CDK7, CCNH, RFC1, RFC2 & RFC4	MLH1, MSH6, 2 & 3	RAD51C, TOP3A	XRCC5

Pathway: Mammalian DNA Repair Pathways. Inputs: BRCA1& ESR1 (ER-α). List of proteins selectively picked from the network, which are associated with both ER-α and BRCA1, with respect to canonical mammalian DDR pathways (HR, NHEJ, MMR BER, NER).

Table S2. Details of the antibodies used in this study

SL No:	Antibody	Catalogue No.	Manufacturer	Dilution
1.	BRCA1	#9010	Cell Signalling Technology	1:100 (IF), (PLA)/1:1000 (WB)
2.	BRCA1	SC D20 #641	Santa Cruz	Co-IP
3.	BRCA1	C11 # SC 514797	Santa Cruz	1:100 (IF/IHC/PLA)
5.	Phospho BRCA1 (Ser1524)	#9009	Cell Signalling Technology	1:100 (IF/IHC)
6.	Phospho BRCA1 (Ser988)	#12888	Santa Cruz	1:100 (IF/IHC) 1:1000 (WB)
7.	ER-α (D8H8)	#8644	Santa Cruz	1:100 (IF/PLA)/1:1000 (WB), 1:50 Co-IP
8.	ER-α (F10)	#8002	Cell Signalling Technology	1:100 (IF/PLA) 1:1000 (WB)
9.	Phospho Histone H2AX (ser139)	#9718	Cell Signalling Technology	1:100 (IF/IHC)/1:1000 (WB)
10.	β-actin	sc-47778	Santacruz	1:1000 (WB)
11.	Histone H3	#9715	Cell Signalling Technology	1:1000 (WB)
12.	P53	#131442	Cell Signalling Technology	1:1000 (WB)
13.	OGG1	Ab 62826	Abcam	1:100 (IF) 1:1000 (WB)
14	OGG1/2 G5	#376937	Santa Cruz	1:100 (IF) 1:1000 (WB)
15.	8-oxoG	#130914	Santa Cruz	1:100 (IF)
16.	8-oxoG	Ab 64548	Abcam	1:100 (IF) 1:1000 (WB)
17.	RAD51 (F11)	#398587	Santa Cruz	1:100 (IF) 1:1000 (WB)
18.	RAD50	#3421	Cell Signalling Technology	1:100 (IF/IHC)/1:1000 (WB)
19.	MRE11	#4895	Cell Signalling Technology	1:100 (IF/IHC)/1:1000 (WB)
20.	NBS1/p95	#3002	Cell Signalling Technology	1:100 (IF/IHC)/1:1000 (WB)
21.	p-CHK2	#2661	Cell Signalling Technology	1:100 (IF)/1:1000 (WB)
23.	53BP1	#4937	Cell Signalling Technology	1:100 (IF/IHC)/1:1000 (WB)
24.	DNA-PK	#4602	Cell Signalling Technology	1:100 (IF)
22.	Ku80	#2753	Cell Signalling Technology	1:100 (IF)/1:1000 (WB)
23.	GFP antibody	SC 8334	Santa Cruz	1:1000 (WB)
24.	p16 INK4A antibody	#4824	Cell Signalling Technology	1:100 (IF)/1:1000 (WB)
25.	p15 INK4B antibody	#4822	Cell Signalling Technology	1:100 (IF)/1:1000 (WB)
26.	PCNA antibody	SC56	Santa Cruz	1:1000 (WB)
27.	ALDH1A1 antibody	#54135	Cell Signalling Technology	1:100 (IF/IHC)
28.	Ki67 antibody	ITEL22027	Immunotag	1:100 (IF)
29.	Mouse anti-Rabbit IgG HRP	sc-2357	Santa Cruz	1:5000 (WB)
30.	Goat anti-Mouse IgG HRP	sc-2005	Santa Cruz	1:5000 (WB)
31.	m-IgGk BP-HRP	sc-516102	Santa Cruz	1:200 (IF)
32.	Bovine anti-Goat IgG HRP	Sc 2378	Santa Cruz	1:200 (IF)
33.	Goat anti-rabbit IgG (Alx 488)	Ab150077	Abcam	1:100 (IF/IHC)
34.	Goat anti-Rabbit IgG FITC	sc-2012	Santa Cruz	1:200 (IF)
35.	Donkey anti-goat IgG FITC	Ab6881	Abcam	1:100 (IF/IHC)
36.	Goat anti-mouse IgG (alx 647)	Ab150115	Abcam	1:100 (IF/IHC)

Immunofluorescence (IF)/Western Blotting (WB)/Immunohistochemistry (IHC)/Proximity Ligation Assay (PLA) and Coimmnoprecipitation.

Table S3. Details of the primers used in this study

Gene	Direction	Sequences
PRIMERS USED FOR qRT-PCR		
BRCA1	Forward (5'-3')	AAGGTTGTTGATGTGGAGGAG
	Reverse (5'-3')	GCCCACGGTAACAACCTCTT
ER-α-1	Forward (5'-3')	GCCAGCAGGTGCCCTACTAC
	Reverse (5'-3')	TGGTACTGGCCAATCTTTCTCTG
ER-α-2	Forward(5'-3')	GATGAGCAACTTGGACAGCAA
	Reverse (5'-3')	CTGGGCTGCTTATCTGGGAAG
OGG1	Forward (5'-3')	GTGCCCGTTACGTGAGTGCCAGTGC
	Reverse (5'-3')	AGAGAAGTGGGGAATGGAGGGGAAGGTG
DNA-PK	Forward (5'-3')	CCAAGTCCAACACCAAGTAGCCACCCA
	Reverse (5'-3')	CCGCCATGCCGCCGAGTCCC
RAD 51	Forward (5'-3')	GGCGGTGAAGGTAAGTGTTTG
	Reverse (5'-3')	CGCTGAGCTATGGATACCATCT
GAPDH	Forward (5'-3')	CAACTACATGGTTTACATGTTC
	Reverse (5'-3')	GCCAGTGGACTCCACGAC
PRIMER FOR HR/NHEJ ASSAY		
DRGFP	Forward (5'-3')	CTGCTAACCATGTTCATGCC
	Reverse (5'-3')	AAGTCGTGCTGCTTCATGTG
LABELLED MODIFIED OLIGOS USED FOR OGG1 ASSAY		
Oligo Name	5' Modification	Sequence
8-oxo-G Wild Type	FITC/6FAM	ATACGCATATACCGCT (G) TCGGCCGATCTCCGAT
8-oxo-G modified	FITC/6FAM	ATACGCATATACCGCT (8-oxo-G) TCGGCCGATCTCCGAT
8-oxo-G complementary		ATCGGAGATCGGCCGA (C) GGCGGTATATGCGTAT

Table S4. Details of the shRNA Plasmids and other constructs used in this study

SL.NO	PLASMID DNA	CAT. NO:
1.	BRCA1 shRNA plasmid	sc-29219-SH SantaCruz
2.	ER-α shRNA plasmid	sc-29305-SH SantaCruz
3.	Control shRNA plasmid	sc-108060 SantaCruz
4.	ERα siRNA (h)	SC-29305 SantaCruz
5.	BRCA1 siRNA (h)	SC-29219 SantaCruz
6.	Control shRNA Plasmid-A	SC37007 SantaCruz
7.	pCAGGS mCherry	#41583 Addgene
8.	pDRGFP	#26475 Addgene
9.	pCBAScel	#26477 Addgene
10.	pEGFP-C1 ER-alpha	#28230 Addgene
11.	pcDNA3 ER alpha	#49498 Addgene
12.	pEGFP-C1	Addgene
13.	pEGFP-N1-p53	#11770 Addgene

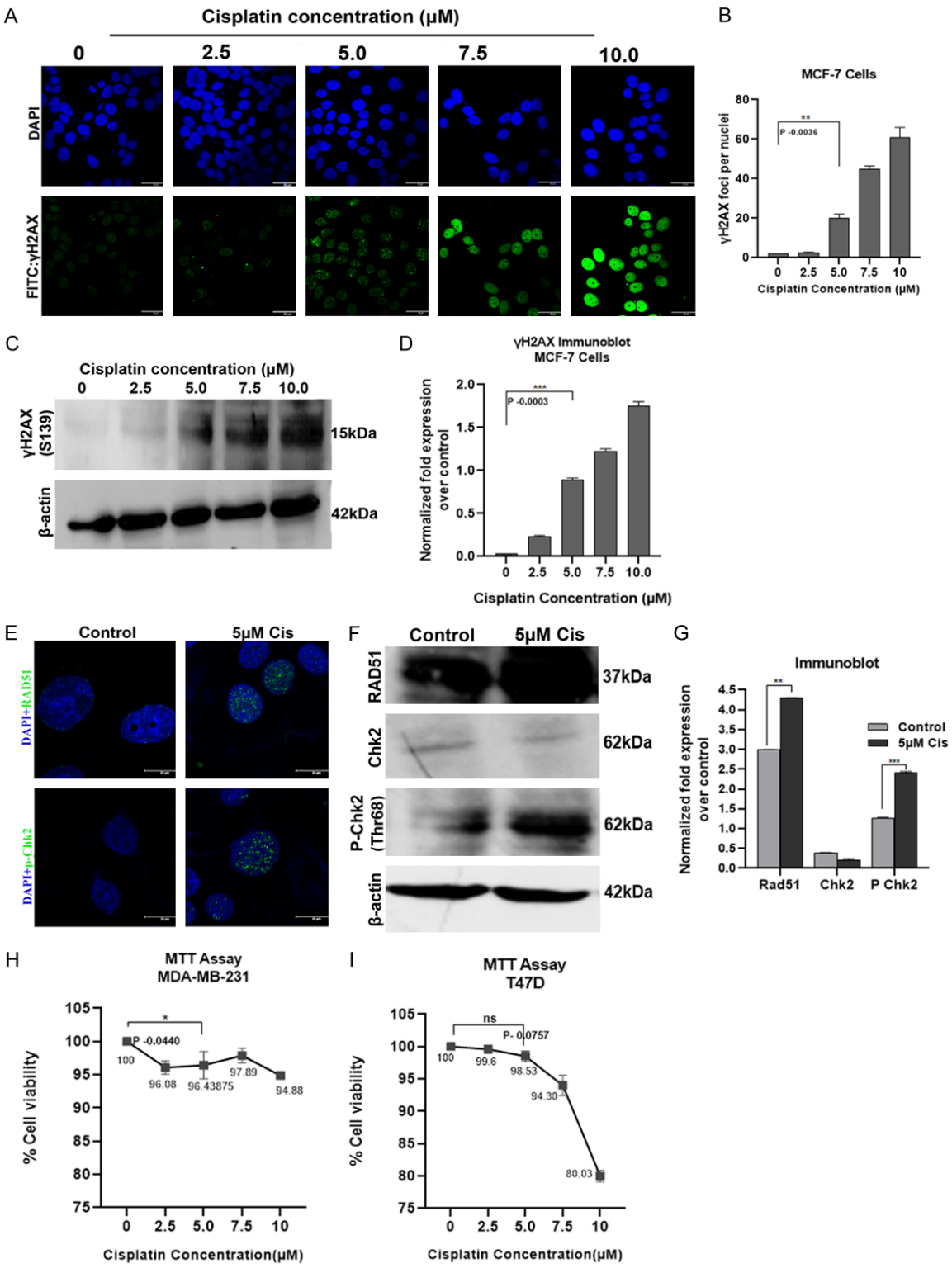

Figure S1. A, B. Immmunofluorescence staining of nuclear γH2AX foci, in response to 5 μM/2 hours cisplatin treatment in MCF-7 cells; 5 μM was found to be the least concentration to induce visible γH2AX in cells. Mean equivalent number of foci per cell was scored, 30 cells per HPF and 10 HPF per sample were scored. C, D. Western blot analysis of γH2AX in MCF-7 cells upon cisplatin induced DSB. E. Immmunofluorescence staining. F, G. Western blot analysis of RAD51 and p-Chk2 upon cisplatin induced DNA-DSB in MCF-7 cells. H, I. Cell proliferation in MDA-MB-231 and T47D cells assessed post cisplatin (0-10 μm) treatment by MTT assay. (60X, Scale bar 20 μm). (Error bars, mean ± SD, *P≤0.05 and **P≤0.005 and as ***P≤0.001, ****P≤0.0001-unpaired t-test).

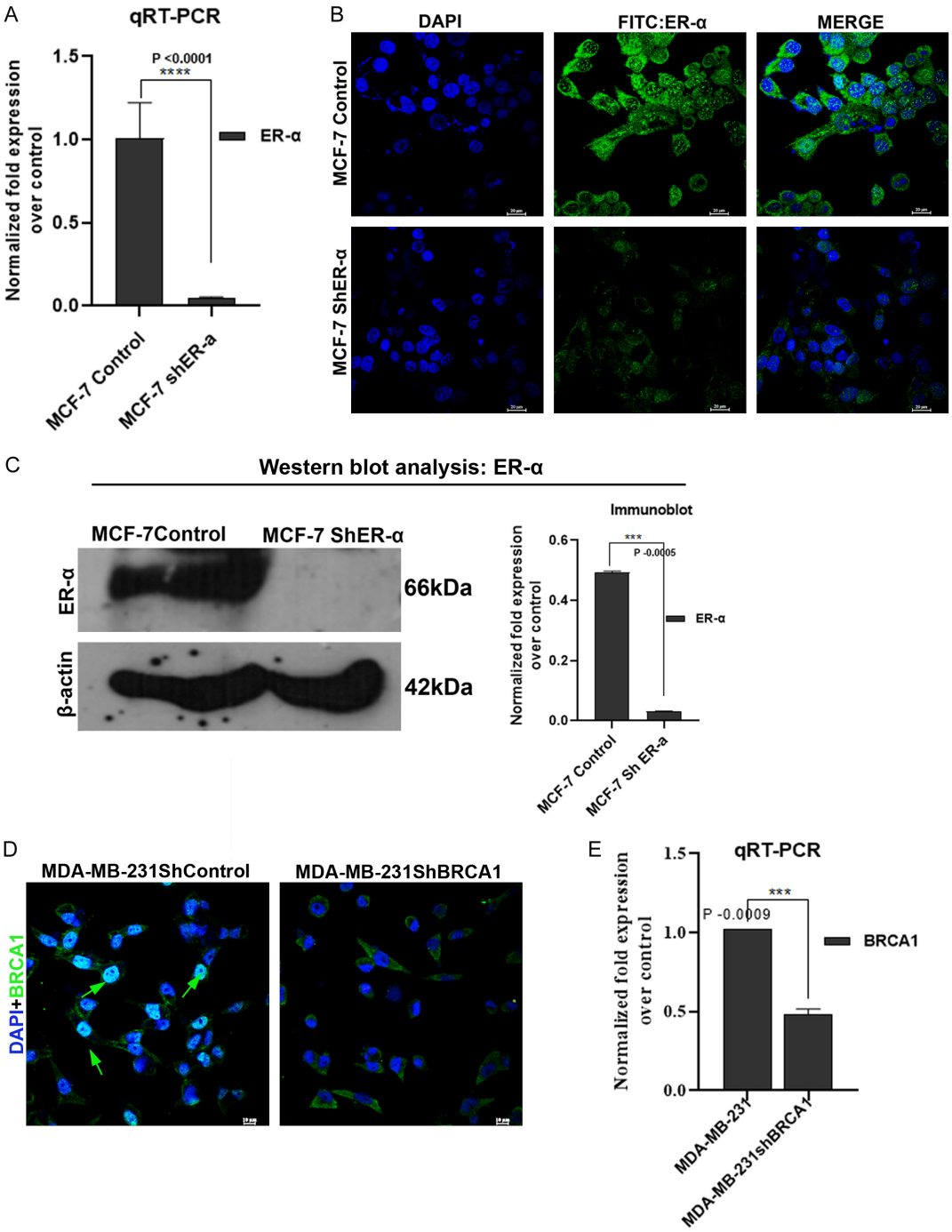
A
qRT-PCR
P <0.0001
****
Normalized fold expression over control
1.5
1.0
0.5
0.0
ER-α
MCF-7 Control
MCF-7 shER-a
B
DAPI
FITC:ER-α
MERGE
MCF-7 Control
MCF-7 ShER-α
C
Western blot analysis: ER-α
MCF-7Control
MCF-7 ShER-α
ER-α
66kDa
β-actin
42kDa
Immunoblot
***
P -0.0005
Normalized fold expression over control
0.6
0.4
0.2
0.0
ER-α
MCF-7 Control
MCF-7 Sh ER-a
D
MDA-MB-231ShControl
MDA-MB-231ShBRCA1
DAPI+BRCA1
E
qRT-PCR
***
P -0.0009
Normalized fold expression over control
1.5
1.0
0.5
0.0
BRCA1
MDA-MB-231
MDA-MB-231shBRCA1

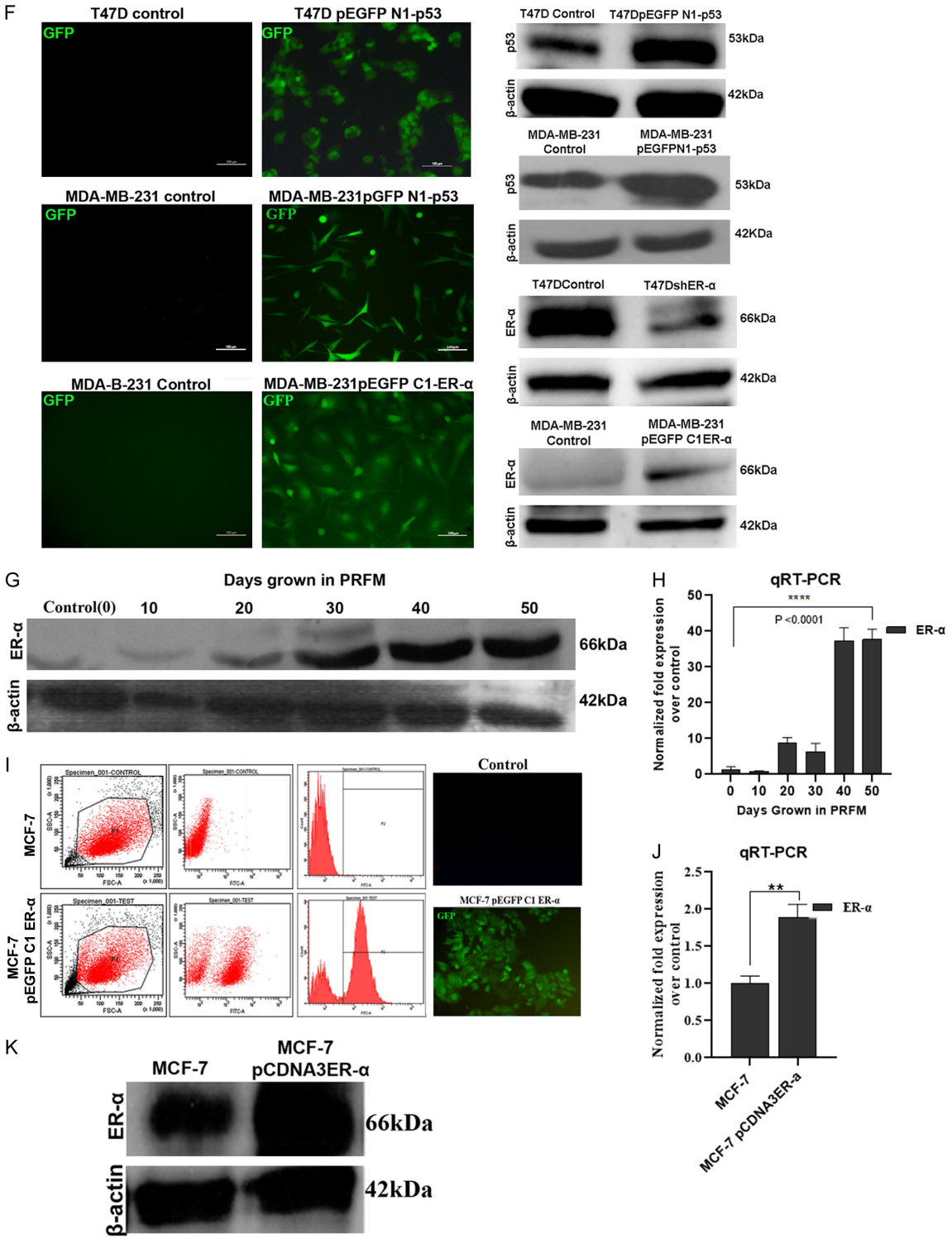

Figure S2. Generation of stable cell lines in breast cancer cell lines using pDNA/shRNA plasmids-detailed in Table S4. (A) qRT-PCR (B) Immmunofluorescence staining and (C) Western blot analysis of mRNA/protein expression of ER-α in MCF-7 cells stably transfected with shER-α plasmid, Scrambled shRNA plasmid (Sh Control) served as the control. (D) Immmunofluorescence staining and (E) qRT-PCR showing the expression of BRCA1 in MDA-MB-231sh-BRCA1 cells in comparison to control cells. (F) Fluorescence (GFP) and western blot images showing the stable transfection of shER-α, pEGFP N1p53 and pEGFPC1 ER-α in T47D and MDA-MB-231 cells. (G) Western blot analysis and (H) qRT-PCR, showing protein/mRNA expression of ER-α, in MCF-7 grown in PRFM (PRFM is the E2 deprived growth media with 5% Charcoal stripped FBS). (I) Flowcytometry analysis of GFP positive MCF-7 cells stably expressing, pEGFPER-α. (J) qRT-PCR and (K) Western blot analysis of, ER-α expression in MCF-7 cells stably expressing pCDNA3ER-α. (Error bars, mean ± SD, *P≤0.05 and **P≤0.005 and as ***P≤0.001, ****P≤0.0001-unpaired t-test).

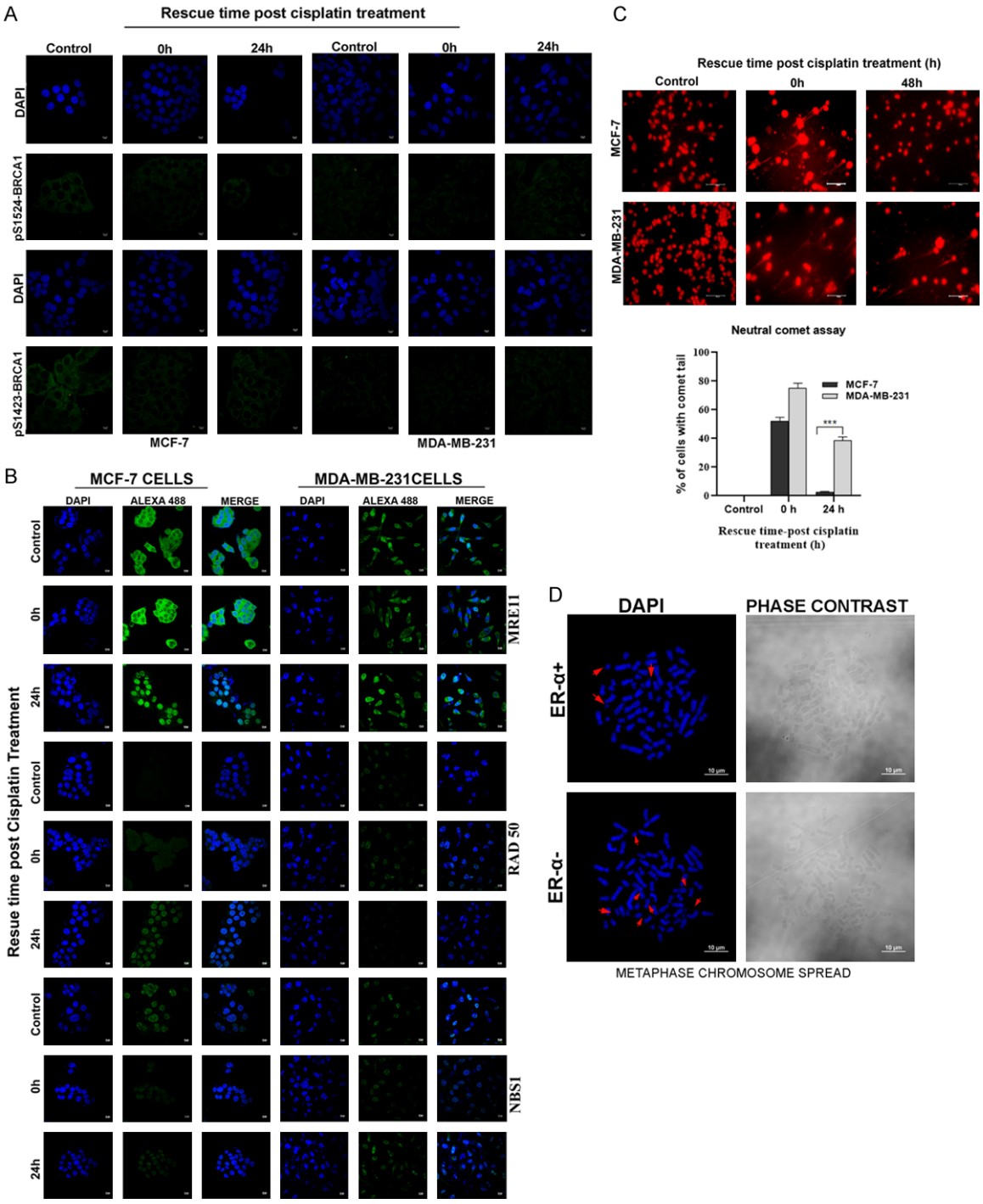

Figure S3. A. Immmunofluorescence staining, for phosphorylated-BRCA1- (p S1524-BRCA1 and p S1423-BRCA1) in response to 5 μM cisplatin induced DNA-DSB, respectively in MCF-7 and MDA-MB-231 cell lines. B. Immmunofluorescence staining of MRN complex proteins (Mre11, Rad50, Nbs1) respectively in MCF-7 and MDA-MB-231 cells in response to 5 μM cisplatin induced DNA-DSB. (60X, Scale bar 10 μm). C. The persistence of comet tails 24 hours post cisplatin treatment in MDA-MB-231 cells in comparison to MCF-7 cells as analyzed by neutral comet assay (Quantification below). D. Representative image of metaphase chromosome spreads of DNA-DSB induced MCF-7 and MDA-MB-231, (red arrows indicate chromosome defects like break, fragmentation etc.). All experiments were performed in triplicates, 5 metaplates were prepared for a single specimen and 10 spreads were analyzed per metaplates. (Error bars, mean ± SD, $^{*}P\leq0.05$ and $^{**}P\leq0.005$ and as $^{***}P\leq0.001$, $^{****}P\leq0.0001$-unpaired t-test).

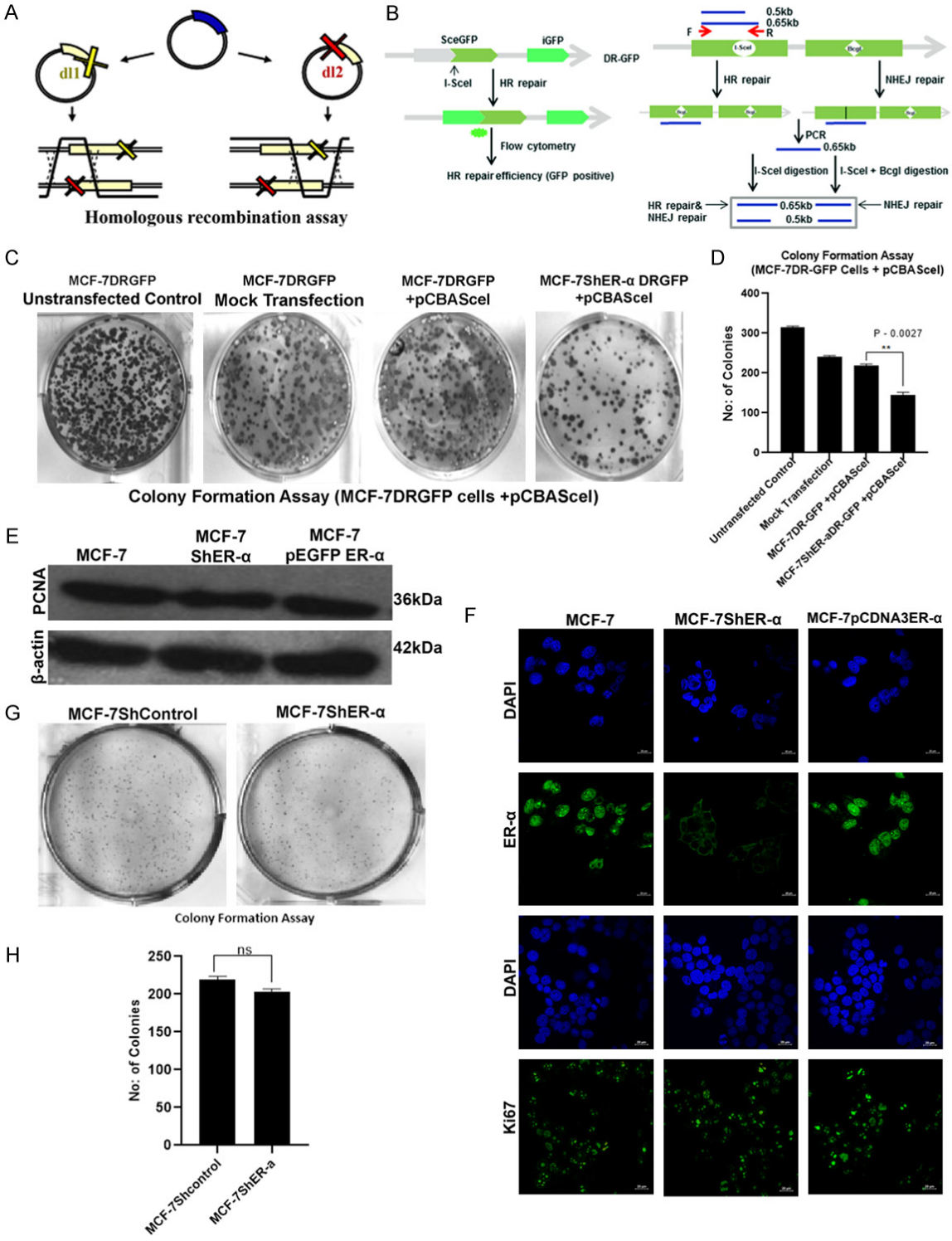

Figure S4. (A) Schematic representation of homologous recombination assay constructs. The lacZα coding region of the positive control plasmid was mutated and two plasmids with different mutations were generated. Therefore, the two plasmids containing different defective lacZα cassettes can form a functional lacZα cassette through intermolecular homologous recombination. The two defective plasmids dI1 and dI2, once cotransfected into cells, will form HR product only if it undergoes homologous recombination and generate the functional lacZα. (B) DR-GFP plasmid is composed of SceI-GFP, whose expression is abolished by an I-SceI endonuclease site within the coding region, and a truncated GFP called iGFP which has a homologous sequence for the SceGFP. I-SceI transfection can cause single DSB in the genome DNA. Once DSB is repaired by HR, GFP will express and can be detected by flow cytometry. PCR was performed using the primer around the I-SceI-induced DSB site with genomic DNA, which was extracted from DR-GFP integrated cells. I-SceI or I-SceI plus BcgI were then used to digest the PCR products. Since

HR repair will replace the I-SceI site with the BcgI site and the NHEJ repair will diminish both enzyme sites, the ratio between uncut DNA and cut DNA after I-SceI digestion represents both HR and NHEJ repair efficiency, while this ratio between them after I-SceI and BcgI digestion reflects only the NHEJ repair efficiency. (Image adopted from Wu. J et al., Molecular cell, 2013 (Wu et al., 2012). (C) Colony Formation Assay and (D) No: of colonies formed by pDRGFP expressing MCF-7 and MCF-7shER-α cells post I-Sce induced DSB. (E) Western blot analysis for the proliferation marker PCNA, in MCF-7, MCF-7shER-α and MCF-7pEGFPER-α cells. (F) Immmunofluorescence staining of Ki67 in MCF-7, MCF-7shER-α and MCF-7pCDNA3ER-α (60X, Scale bar 20 μm). (G, H) Colony Formation Assay showing the No: of colonies formed by MCF-7 and MCF-7shER cells.

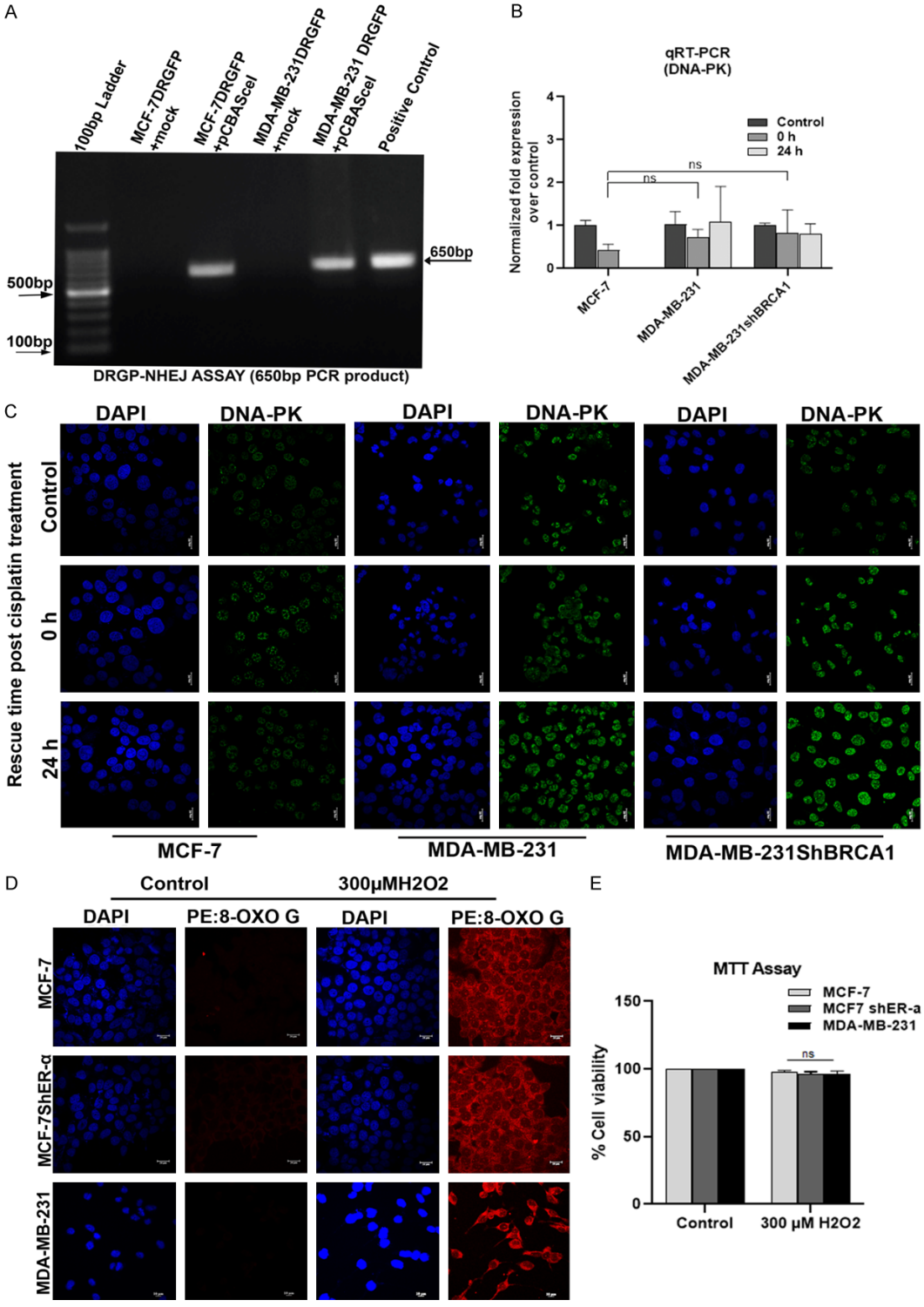

Figure S5. DR-GFP-integrated MCF-7 and MDA MB-231 cells were transfected with mock or I-SceI, 48 hours post transfection, genomic DNA was extracted for PCR amplification and (A) is the representative agarose gel image showing the 650 bp PCR amplicon. (B) qRT-PCR and (C) Immmunofluorescence staining of DNA-PK in DNA-DSB induced, MCF-7, MDA-MB-231 and MDA-MB-231shBRCA1 cells. (60X, Scale bar 20 μm). (D) Immmunofluorescence staining of 8-OXO-G lesions in MCF-7, MCF-7shERα and MDA-MB-231 cells treated with 300 μM H_2O_2 for 30 minutes, (60X, Scale bar 10 μm). (E) Percentage cell viability, of MCF-7, MCF-7shERα and MDA-MB-231 cells upon 300 μM H_2O_2 treatment, as analyzed by MTT assay. 300 μM did not significantly affect the cell proliferation.

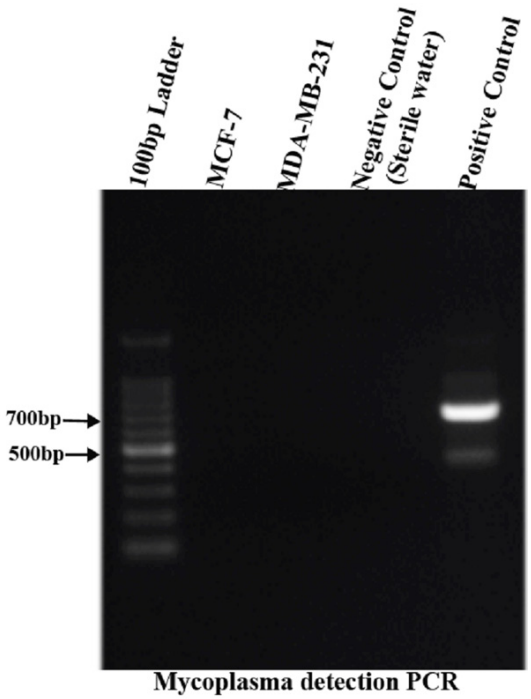

Figure S6. Represents the mycoplasma detection PCR; The cell lines used in the study as well as the growth media were examined for mycoplasma contamination using the GPO1, MGSO primers, with sterile water as negative and mycoplasma DNA as the positive controls.